

[View the Full Text HTML](#)



## Isomerization Dynamics and Control of the $\eta^2/N$ Equilibrium for Pyridine Complexes

David A. Delafuente,<sup>†</sup> George W. Kosturko,<sup>†</sup> Peter M. Graham,<sup>†</sup> W. Hill Harman,<sup>†</sup> William H. Myers,<sup>‡</sup> Yogesh Surendranath,<sup>†</sup> Rachel C. Klet,<sup>†</sup> Kevin D. Welch,<sup>†</sup> Carl O. Trindle,<sup>†</sup> Michal Sabat,<sup>†</sup> and W. Dean Harman\*<sup>†</sup>

Contribution from the Department of Chemistry, University of Virginia, Charlottesville, Virginia 22904-4319, and Department of Chemistry, University of Richmond, Richmond, Virginia 23173

Received September 19, 2006; E-mail: wdh5z@virginia.edu

**Abstract:** A series of pyridine complexes are prepared of the general form  $\text{TpW}(\text{NO})(\text{PMe}_3)(\text{pyr})$  where pyr is either pyridine or a substituted pyridine. Depending on substitution pattern, the pyridine can be either N- or  $\eta^2$ -coordinated, and the role of the pyridine substituents and metal oxidation state in determining this equilibrium is explored. For  $\eta^2$ -pyridine complexes, the substituent pattern and solubility characteristics also determine the ratio of coordination diastereomers. Rates of both intra- and interfacial linkage isomerizations are explored along with the pyridine rotational barrier. This study is supported by DFT calculations and X-ray data and includes characterization of both  $\eta^2$ -pyridine and  $\eta^2$ -pyridinium complexes.

### Introduction

Though inherently inert, arenes may be activated by their coordination to a transition metal. This is generally accomplished with electron deficient complexes that bind the arene with maximum hapticity.<sup>1–4</sup> Alternatively, the arene can bind through fewer atoms of the ring, resulting in a disruption of the aromatic character of the ligand.<sup>5–8</sup> Pyridines, like their carbocyclic counterparts, readily form complexes with transition metals, but they typically bind through nitrogen. Reports of  $\eta^6$ - and  $\eta^2$ -bound pyridine complexes have emerged,<sup>9–18</sup> but little is known

about the modulated ligand reactivity effected by the metal.<sup>19</sup> Recently, the complex  $\text{TpW}(\text{NO})(\text{PMe}_3)(\eta^2\text{-benzene})$  was reported to react with either 2,6-lutidine or 2-(dimethylamino)pyridine (2-DMAP) to form  $\eta^2$ -bound pyridine complexes. Coordinated to tungsten in this manner, these pyridines are transformed into 2-azadienes and participate in Diels–Alder reactions to form isoquinuclidine cores.<sup>20</sup> The parent pyridine also forms a complex with  $\{\text{TpW}(\text{NO})(\text{PMe}_3)\}$ , but in this case the heterocycle is bound through nitrogen (*vide infra*) and as such is unreactive toward cycloaddition. Given the potential of  $\eta^2$ -pyridine complexes in alkaloid synthesis,<sup>20</sup> we felt it would be valuable to explore the N/ $\eta^2$  equilibrium for  $\text{TpW}(\text{NO})(\text{PMe}_3)(\text{pyridine})$  and its dependence on the heterocycle substituents and metal oxidation state. Furthermore, in cases where  $\eta^2$ -coordination is observed, we hoped to develop a strategy for controlling the stereochemistry of coordination, which could lead to enantioenriched bicyclic alkaloids.<sup>20</sup>

### Results and Discussion

Our investigation commenced with a comprehensive study of the parent pyridine complex,  $\text{TpW}(\text{NO})(\text{PMe}_3)(\text{pyridine})$  (**2**). A DME solution was prepared of pyridine and the benzene complex,  $\text{TpW}(\text{NO})(\text{PMe}_3)(\eta^2\text{-benzene})$  (**1**).<sup>21</sup> The solution color soon turned from pale yellow to deep turquoise. Upon addition of the reaction mixture to pentane, the complex **2** was isolated in 60% yield.<sup>22</sup> A cyclic voltammogram of **2** reveals a reversible

- <sup>†</sup> University of Virginia.  
<sup>‡</sup> University of Richmond.
- (1) Kündig, E. P. *Transition Metal Arene  $\pi$  Complexes in Organic Synthesis and Catalysis*; Springer-Verlag: Berlin, 2004.
  - (2) Pape, A. R.; Kaliappan, K. P.; Kündig, E. P. *Chem. Rev.* **2000**, *100*, 2917–2940.
  - (3) Semmelhack, M. F. In *Comprehensive Organometallic Chemistry II*; Abel, E. W., Stone, F. G. A., Wilkinson, G., Eds.; Pergamon Press: Oxford, UK, 1995; Vol. 12, pp 979–1015.
  - (4) Semmelhack, M. F. *Transition Metal Arene Complexes: Ring Lithiation*; Pergamon: Oxford, 1995; Vol. 12.
  - (5) Keane, J. M.; Harman, W. D. *Organometallics* **2005**, *24*, 1786–1798.
  - (6) Park, S. K.; Geib, S. J.; Cooper, N. J. *J. Am. Chem. Soc.* **1997**, *119*, 8365–8366.
  - (7) Thompson, R. L.; Lee, S.; Rheingold, A. L.; Cooper, N. J. *Organometallics* **1991**, *10*, 1657–1659.
  - (8) Harman, W. D. *Chem. Rev.* **1997**, *97*, 1953–1978.
  - (9) Davies, S. G.; Shipton, M. R. *J. Chem. Soc., Chem. Commun.* **1989**, 995–996.
  - (10) Fish, R. H.; Kim, H. S.; Fong, R. H. *Organometallics* **1989**, *8*, 1375–1377.
  - (11) Wucherer, E. J.; Muetterties, E. L. *Organometallics* **1987**, *6*, 1691–1695.
  - (12) Meiere, S. H.; Brooks, B. C.; Gunnoe, T. B.; Sabat, M.; Harman, W. D. *Organometallics* **2001**, *20*, 1038–1040.
  - (13) Cordone, R.; Harman, W. D.; Taube, H. *J. Am. Chem. Soc.* **1989**, *111*, 2896–2900.
  - (14) Cordone, R.; Taube, H. *J. Am. Chem. Soc.* **1987**, *109*, 8101–8102.
  - (15) Bonanno, J. B.; Viege, A. S.; Wolczanski, P. T.; Lobkovsky, E. B. *Inorg. Chim. Acta* **2003**, *345*, 173–184.
  - (16) Kleckley, T. S.; Bennett, J. L.; Wolczanski, P. T.; Lobkovsky, E. B. *J. Am. Chem. Soc.* **1997**, *119*, 247–248.
  - (17) Covert, K. J.; Neithamer, D. R.; Zonneville, M. C.; LaPointe, R. E.; Schaller, C. P.; Wolczanski, P. T. *Inorg. Chem.* **1991**, *30*, 2493–2508.

- (18) Neithamer, D. R.; Parkanyi, L.; Mitchell, J. F.; Wolczanski, P. T. *J. Am. Chem. Soc.* **1988**, *110*, 4421–4423.
- (19) Davies, S. G.; Edwards, A. J.; Shipton, M. R. *J. Chem. Soc., Perkin Trans. I* **1991**, 1009–1017.
- (20) Graham, P. M.; Delafuente, D. A.; Liu, W.; Sabat, M.; Harman, W. D. *J. Am. Chem. Soc.* **2005**, *127*, 10568–10572.
- (21) Graham, P.; Meiere, S. H.; Sabat, M.; Harman, W. D. *Organometallics* **2003**, *22*, 4364–4366.
- (22) This complex reacts violently with oxygen even as a solid and must be kept under inert atmosphere.

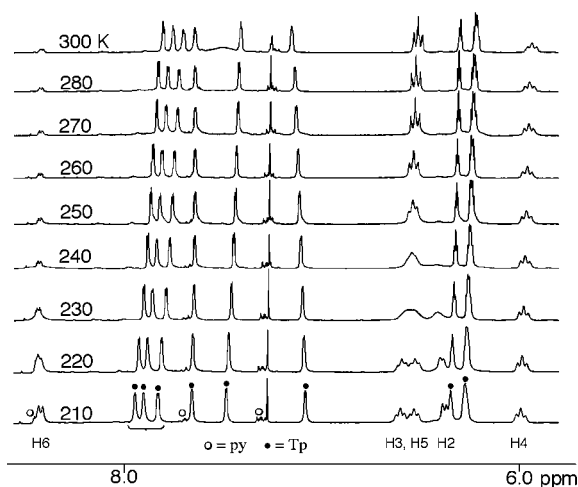


**Figure 1.** Variable temperature  $^1\text{H}$  NMR spectra of compound **2**.

couple at  $-0.78$  V corresponding to its  $I/O$  reduction potential. Infrared data for **2** shows a  $\nu(\text{NO})$  at  $1503\text{ cm}^{-1}$ , an astonishingly low value for a terminal NO.<sup>23</sup> The  $^1\text{H}$  NMR of **2** has three broad but distinct pyridine resonances at  $22^\circ\text{C}$  as a result of a hindered rotation about the pyridine  $\text{N}-\text{W}$  bond.<sup>24</sup>  $^1\text{H}$  NMR spectra were recorded from 300 to 210 K (Figure 1). At the lowest temperature, the triplet observed at 6.57 ppm at  $20^\circ\text{C}$  is resolved into two distinct resonances at 6.61 and 6.69 ppm, and the broad peak at 7.5 ppm is replaced by two doublets at 8.59 (overlapping with free pyridine) and 6.45 ppm. The large difference in chemical shift between the H2 and H6 protons is consonant with shielding of H2 resulting from its location between two of the pyrazolyl rings.<sup>25</sup> Protons H3, H4, and H5 are shifted well upfield compared to free pyridine, suggesting a significant amount of electron donation from the metal. A coalescence temperature was identified at 230 K, corresponding to a rotational free energy barrier of  $\Delta G^\ddagger = 11$  kcal/mol.

To understand the origin of the pyridine rotational barrier and to determine the likelihood of  $\eta^2$  coordination for the pyridine complex **2**, various isomers were modeled using the Gaussian 03 program suite.<sup>26</sup> Relative energies were determined using a hybrid density functional B3LYP expressed in a hybrid basis. The basis incorporates the Los Alamos pseudopotential LANL2DZ and the associated basis functions<sup>27–29</sup> for tungsten and Pople's 6-31G(d) basis for all other atoms.<sup>30</sup> This combination has proved reliable for Os, Mo, Re, and W systems for relative (binding) energies, charge transfer, and preferred structures, especially in similar systems.<sup>31</sup> These results (Figure 2) show that the preferred orientation of the N-bound pyridine roughly aligns the pyridine plane with the  $\text{W}-\text{NO}$  axis ( $\text{N}_{\text{NO}}-\text{W}-\text{N}_{\text{pyr}}-\text{C} = 17^\circ$ ), while the rotational transition state (**T**, Figures 2 and 3) roughly aligns the pyridine plane with the

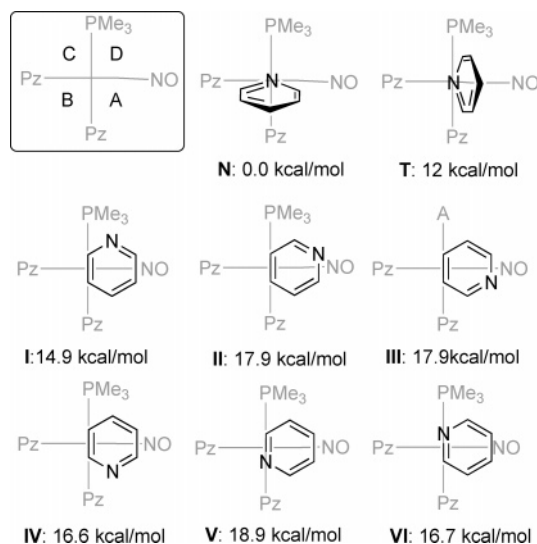


**Figure 2.** Calculated energies for  $N$ - and  $\eta^2$ -coordinated pyridine complexes (**2**). The perspective view is looking down the pyridine–metal bond axis.

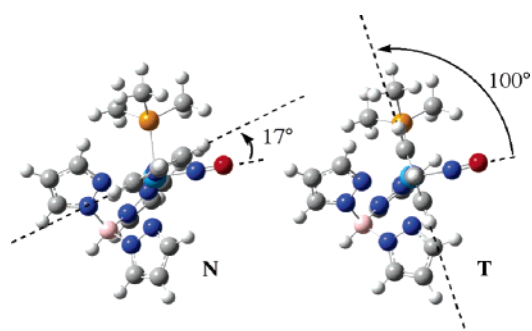


**Figure 3.** Equilibrium (**N**) and transition state (**T**) energies for  $N$ -bound pyridine complex **2**. The perspective view is looking down the pyridine–metal bond axis.

$\text{W}-\text{PMe}_3$  axis, ( $\text{N}_{\text{NO}}-\text{W}-\text{N}_{\text{pyr}}-\text{C} = 100^\circ$ ). This transition state lies 12.3 kcal/mol above the equilibrium form (**N**), which is favored by about 15 kcal over any of the  $\eta^2$ -bound isomers (**I**–**VI**). Of the  $\eta^2$  species, only those in which the aromatic ring extends over quadrants D and A were considered. The most stable orientation is predicted to be that with the metal bound 2,3- $\eta^2$  and the nitrogen oriented toward the  $\text{PMe}_3$  (**I**). This form is about 2 kcal more stable than its stereoisomer (**IV**) in which the nitrogen is oriented away from the  $\text{PMe}_3$ . There is virtually no difference in energy between the 3,4- $\eta^2$  coordination diastereomers (**II**, **III**).

As has been previously described,<sup>20</sup> the lutidine complex (**3**) differs dramatically in color, electrochemistry, and spectroscopy, from the  $N$ -bound pyridine complex (**2**). Complex **3** exists in solution as a 3:1 equilibrium mixture of the C3,C4- $\eta^2$  species **3B** and its 4-lutidinyl hydride isomer (**3H**) (Scheme 1). The  $\eta^2$ -lutidine (**3B**) shows an  $E_{\text{p,a}} = -0.07$  V, about 700 mV positive of the formal reduction for **2**, and a  $\nu(\text{NO})$  in the infrared absorption spectrum at  $1565\text{ cm}^{-1}$ , over  $60\text{ cm}^{-1}$  blue-shifted from **2**. The  $^1\text{H}$  NMR spectrum of **3B** includes two upfield resonances at 2.25 and 4.11 ppm corresponding to the protons belonging to the bound carbons.<sup>32</sup> The 4-lutidinyl hydride (**3H**) is identified by a  $\text{W}-\text{H}$  signal at 8.93 ppm, split into a doublet ( $J_{\text{PH}} = 99.5$  Hz). This hydride signal has  $^{183}\text{W}$

(23) Burkey, D. J.; Debad, J. D.; Legzdins, P. *J. Am. Chem. Soc.* **1997**, *119*, 1139–1140.

(24) The pyridine complex **2** and other  $N$ -coordinated pyridine complexes described herein have reduction potentials similar to cobaltocene. Exposure to even trace amounts of an oxidant (e.g. air, water) will wipe out the NMR signals.

(25) Meiere, S. H.; Harman, W. D. *Organometallics* **2001**, *20*, 3876–3883.

(26) Frisch, M. J. et al. Gaussian 03, Revision C.02, Gaussian, Inc., Wallingford CT, 2004.

(27) Hay, P. J.; Wadt, W. R. *J. Chem. Phys.* **1985**, *82*, 270–274.

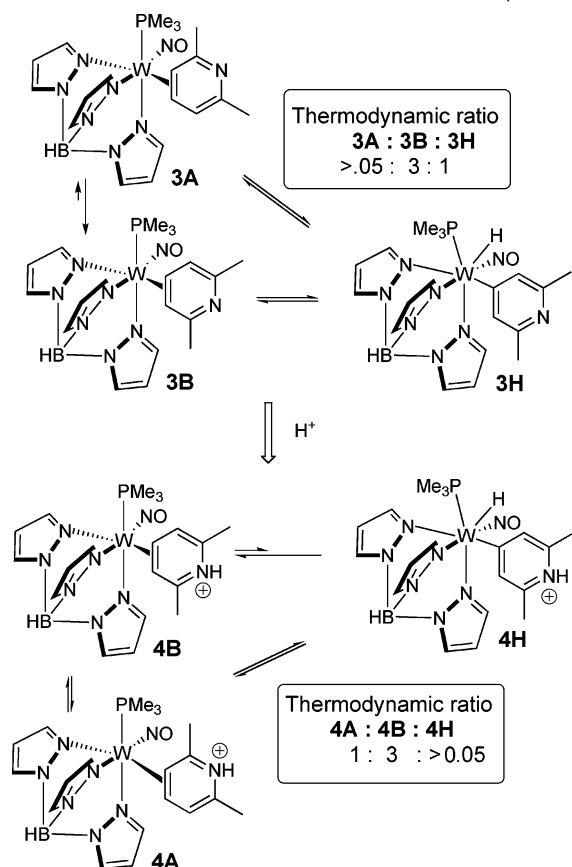
(28) Wadt, W. R.; Hay, P. J. *J. Chem. Phys.* **1985**, *82*, 284–298.

(29) Hay, P. J.; Wadt, W. R. *J. Chem. Phys.* **1985**, *82*, 299–310.

(30) Rassolov, V. A.; Ratner, M. A.; Pople, J. A.; Redfern, P. C.; Curtiss, L. A. *J. Comput. Chem.* **2001**, *22*, 976–991.

(31) Trindle, C. O.; Harman, W. D. *J. Comput. Chem.* **2005**, *26*, 194–200.

(32) At  $22^\circ\text{C}$ , these peaks are well resolved, indicating that any fluxional process (e.g., “ring-whizzing”) is slower than the NMR measurement (300 MHz).

**Scheme 1.** Formation and Protonation of Lutidine Complex

satellites appearing as a dd ( $J_{\text{PH}} = 99.5$ ,  $J_{\text{WH}} = 32.8$  Hz). Over a period of several hours, signals for the equilibrated isomers **3B** and **3H** are replaced by those of the acetone complex  $\text{TpW}(\text{NO})(\text{PMe}_3)(\eta^2\text{-acetone})$ .<sup>33</sup> The mixture of lutidine (**3B**) and lutidinyl hydride (**3H**) complexes readily protonate in THF to produce conjugate acids  $\text{TpW}(\text{NO})(\text{PMe}_3)(\eta^2\text{-lutidinium})(\text{OTf})$  (**4B**) and  $\text{TpW}(\text{NO})(\text{PMe}_3)(\text{H})(4\text{-lutidinyl})\cdot\text{HOTf}$  (**4H**), initially observed as a 3:1 ratio. When a solution of **3B** and **3H** are quantitatively precipitated from solution with pentane, the hydride converts back to the  $\eta^2$ -aromatic form (**3B**). If the resulting *solid* sample of **3B** is added directly to an acidic solution of acetone- $d_6$ , the  $\eta^2$ -lutidinium **4B** is the only species observed by  $^1\text{H}$  NMR. Over a period of 18 h, a new isomer appears (**4A**) that is spectroscopically consistent with the coordination isomer of **4B** (see Scheme 1). The equilibrium ratio of **4A**:**4B** is 1:3 with only trace amounts of **4H** (<5%) present. Upon deprotonation of compound **4**, only compounds **3B** and **3H** are immediately observed by  $^1\text{H}$  NMR (<5 min) in their thermodynamic equilibrium of 3:1 (**B**:**H**). Taken together, these observations support the following conclusions at ambient temperature: (1) The isomerization between the two  $\eta^2$ -bound pyridine coordination diastereomers occurs rapidly ( $t_{1/2} < 5$  min). Given that the NMR spectrum at this temperature is not broadened, we can estimate the free energy of activation as being in the range of 15–19 kcal/mol.<sup>34</sup> (2) The C–H oxidative addition of an  $\eta^2$ -pyridine complex is both rapid ( $t_{1/2} < 5$  min) and reversible. (3) The corresponding isomerization between

two lutidinium diastereomers and conversion of these  $\eta^2$ -isomers to the protonated lutidinyl hydride (**4H**) is considerably slower ( $t_{1/2}$  of several hours). (4) Addition of pentane to a solution of lutidinyl hydride **3H** induces its conversion to the  $\eta^2$  isomer **3B** through its precipitation (CIDR).<sup>35</sup>

Related to these findings are reports of  $\{\text{W}(\text{PMe}_3)_5\}$ ,<sup>36</sup>  $\text{Y}(\text{py})_6(\text{Me})$ ,<sup>37</sup> and,  $\text{Ta}(\text{silox})_3$ <sup>17</sup> inserting into the C–H bond of a pyridine. Of note, for the  $\text{Ta}(\text{silox})_3(\text{lutidine})$  system, the oxidative addition across the C4–H bond is also reversible and actually *precedes* the formation of the  $\eta^2$ -isomer lutidine isomer, which appears hours later (25 °C).<sup>17</sup>

A landmark study by Wolczanski et al., examined factors that influence N vs  $\eta^2$ -pyridine coordination for  $d^2$  systems of the type  $\text{M}(\text{silox})_3$  ( $\text{M} = \text{Ta}, \text{Ti}, \text{Sc}, \text{V}$ ).<sup>17</sup> One of the aims of the present study is to survey a collection of common pyridines for the  $[\text{TpW}(\text{NO})(\text{PMe}_3)]^{n+}$  ( $n = 0, 1$ ) systems with different substituents and substitution patterns in order to identify what attributes of the ligand and oxidation state could influence the pyridine binding mode. In consideration of the extraordinarily air-sensitive nature of the N-bound pyridine complexes (*vide supra*), we found it most convenient to probe for the binding mode using cyclic voltammetry. While color is also a convenient indicator (N complexes are dark green to blue), the intense absorption of an N-coordinated pyridine would determine the appearance of the solution, even if it were formed in minute amounts. Solutions were prepared of the benzene complex (**1**), dissolved in a minimum amount of the pyridine (Table 1), and after 18 h, a sample of each solution was evaluated by cyclic voltammetry. In some cases, a cyclic voltammogram of the reaction mixture showed a chemically reversible couple near  $-0.9$  V ( $\pm \sim 100$  mV; Table 1). These observations were taken to signal the formation of N-bound pyridine complexes similar to **2**, and for these complexes (**2–9**) isolation was not attempted. However, other reaction mixtures showed a large anodic wave near 0.0 V ( $\pm \sim 100$  mV) at a scan rate of 100 mV/s, similar to that observed for the lutidine complex **3**. The results of this electrochemical survey are summarized in Table 1. In general, complexes with  $\pi$  electron-releasing groups at the 2, 4, or 6 positions have potentials shifted about 100 mV negative of their 3- or 5-substituted or alkylated analogues for both N and  $\eta^2$ -bound species, indicating their increased tendency to become oxidized. Complexes that showed promise as  $\eta^2$ -pyridine complexes (**10–15**) were prepared on a synthetic scale, isolated, and characterized, as described below. In the case of the 2,6-diacetylpyridine complex, an anodic wave occurs at 0.35 V, significantly positive to that found with the other reactions. This observation along with spectroscopic data<sup>38</sup> indicates that a *carbonyl* is coordinated, not the pyridine ring.

In Tables 2 and 3,  $^1\text{H}$  and  $^{13}\text{C}$  NMR data are listed for the  $\eta^2$ -complexes **10–15**. Assignments of regio- and stereochemistry (shown in Figure 4) were made using COSY, HSQC, and HMBC data, and thorough comparison with data in Tables 2 and 3. The four isomer classes observed are designated in Table 2; in no case was the metal found coordinated across a N=C

(33) Graham, P. M.; Mocella, C. J.; Sabat, M.; Harman, W. D. *Organometallics* **2005**, *24*, 911–919.

(34) Brooks, B. C.; Meiere, S. H.; Friedman, L. A.; Carrig, E. H.; Gunnoe, T. B.; Harman, W. D. *J. Am. Chem. Soc.* **2001**, *123*, 3541–3550.

(35) Keane, J. M.; Ding, F.; Sabat, M.; Harman, W. D. *J. Am. Chem. Soc.* **2004**, *126*, 785–789.

(36) Zhu, G.; Tanski, J. M.; Churchill, D. G.; Janak, K. E.; Parkin, G. J. *Am. Chem. Soc.* **2002**, *124*, 13658–13659.

(37) Arndt, S.; Elvidge, B. R.; Zeimentz, P. M.; Spaniol, T. P.; Okuda, J. *Organometallics* **2006**, *25*, 793–795.

(38) Key features include uncomplexed pyridine proton resonances between 7.7 and 7.1 ppm, and an NO stretch at 1597  $\text{cm}^{-1}$ .

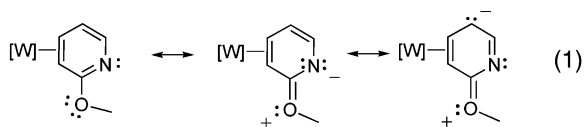


**Table 1.** Coordination Mode of Pyridine Complexes and Their Electrochemical Potentials

| Compound Number | $\eta^1$ -Bound | $E_{1/2}$ <sup>a</sup> | Compound Number | $\eta^2$ -Bound | $E_{p,a}$ <sup>a,b</sup> |
|-----------------|-----------------|------------------------|-----------------|-----------------|--------------------------|
| 2               |                 | -0.78                  | 3               |                 | -0.07                    |
| 5               |                 | -0.80                  | 10              |                 | -0.18                    |
| 6               |                 | -0.78                  | 11              |                 | -0.06                    |
| 7               |                 | -0.93                  | 12              |                 | -0.18                    |
| 8               |                 | -1.04                  | 13              |                 | 0.03                     |
| 9               |                 | -0.73                  | 14              |                 | 0.08                     |
|                 |                 |                        | 15              |                 | -0.10                    |

<sup>a</sup> Values are reported vs NHE. <sup>b</sup> Values are reported for  $E_{p,a}$  at 100 mV/s. [W] = TpW(NO)(PMe<sub>3</sub>).

bond, the mode seen for d<sup>2</sup> systems.<sup>17,18,39</sup> In general, hydrogens associated with carbons directly adjacent to nitrogen show the most downfield resonances, and the most shielded ring proton is always that in quadrant B (see Figure 2), a result of being located between two pyrazole rings.<sup>40</sup> Notably, the large differences in chemical shifts for the ring protons along with COSY and NOESY data to determine the vicinal proton sequence allow for the unambiguous determination of isomer class.



Both steric and electronic properties of the pyridine substituents influence whether the pyridine binds N or  $\eta^2$  to the tungsten. The most obvious feature in Table 1 is the requirement of at least one substituent on a carbon adjacent to the nitrogen. In some cases, this effect can be purely steric such as the *tert*-butyl group in **15** or the TMS group in **13**. Alternatively, if the 2-substituent is a  $\pi$ -donating group, such as a methoxy or amino group,  $\eta^2$ -coordination is also observed (e.g., **11**, **12**). We note that for the methoxy group, the steric effect alone is not sufficient. Consider the case of 2-ethylpyridine, which forms an N-bound complex (**5**) even though the ethyl substituent has a larger steric profile than a methoxy group. Coordination of the metal at C3 and C4 of the 2-methoxypyridine reduces the

**Table 2.** Proton Data for Compounds **3** and **10–15** Reported in ppm (See Figure 2 for full stereochemistry) and Average (or Expected) Values

|            | proton resonance (ppm)                         |      |      |      |       |
|------------|--|------|------|------|-------|
|            | a  | b    | c    | d    | e     |
| class III  |  |      |      |      |       |
| <b>3B</b>  | -  | 2.25 | 4.11 | 6.03 | -     |
| <b>10B</b> | -  | 2.08 | 4.17 | 5.22 | -     |
| <b>11B</b> | -  | 2.26 | 3.98 | 6.02 | 6.39  |
| <b>12B</b> | -  | 2.12 | 4.03 | 5.73 | 6.45  |
| <b>13B</b> | 8.39   | 2.20 | 3.88 | 6.95 | -     |
| <b>14B</b> | 8.77   | 2.32 | 3.79 | 6.70 | -     |
| <b>15B</b> | 8.63   | 2.21 | 4.00 | 6.4  | -     |
| class II   |  |      |      |      |       |
| <b>10A</b> | -  | 3.67 | 2.23 | 5.45 | -     |
| <b>11A</b> | -  | 3.62 | 2.26 | 6.42 | 6.41  |
| <b>13A</b> | 8.55   | 3.88 | 2.16 | 6.71 | -     |
| <b>15A</b> | 8.42   | 3.82 | n.o. | 6.50 | -     |
| class I    |  |      |      |      |       |
| <b>15C</b> | -  | 5.82 | 7.46 | 2.07 | 5.73  |
| class IV   |  |      |      |      |       |
| <b>15D</b> | 4.20   | 3.62 | 7.4  | 5.85 | -     |
|            | average values, and estimates (in parentheses) |      |      |      |       |
|            | a  | b    | c    | d    | e     |
| class I    | (8.5)  | 5.8  | 7.5  | 2.1  | 5.7   |
| class II   | 8.4  | 3.7  | 2.2  | 6.3  | 6.4   |
| class III  | 8.6  | 2.2  | 4.0  | 6.1  | 6.4   |
| class IV   | 4.2  | 3.6  | 7.4  | 5.9  | (8.5) |

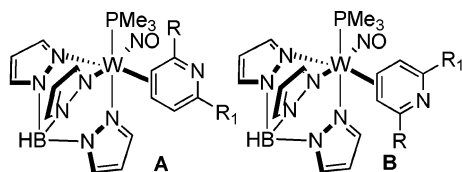
cross conjugation and enhances the interaction of the methoxy group with the 2-azadiene character of the uncoordinated portion of the pyridine.

Interestingly, the electronic stabilization afforded by a methoxy group in the 2-position is not sufficient to induce  $\eta^2$ -coordination in the 4-methoxypyridine (**7**) or 4-(dimethylamino)pyridine (DMAP) (**8**) complexes, even though similar resonance stabilization arguments could be made if the metal were bound 5,6- $\eta^2$ . Diastereomer ratios for complexes **3**, **10–15** are summarized in Figure 4.

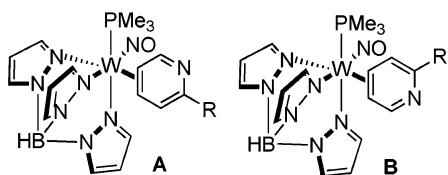
In order to examine how a  $\pi$ -withdrawing group affects coordination of the tungsten, we desired a 2-acetylpyridine complex. However, complexation of 2,6-diacetylpyridine occurs through the acetyl group, and this was expected for 2-acetylpyridine as well. Therefore, the pyridine acetal was first prepared and then complexed to form **14**, isolated from solution as a single diastereomer (**14B**). The acetal complex **14B** can be protonated with  $\text{p}^+\text{HOTf}$  in acetone to produce TpW(NO)(PMe<sub>3</sub>)( $\eta^2$ -4,5-(2-(2-methyl-1,3-dioxolan-2-yl)-pyridinium)-(OTf)) (**16B**) in 72% yield, isolated as a single diastereomer (Scheme 2). If **16B** is deprotonated, only compound **14B** is observed kinetically but this complex isomerizes to a 1:1 ratio of coordination diastereomers **14A**:**14B** within 1.5 h. The acetyl protecting group can be removed by addition of HOTf and water in acetonitrile to produce TpW(NO)(PMe<sub>3</sub>)( $\eta^2$ -2-acetylpyridinium) (**17B**) in 76% yield. Unfortunately, at room-temperature

(39) Fox, P. A.; Bruck, M. A.; Gray, S. D.; Gruhn, N. E.; Grittini, C.; Wigley, D. E. *Organometallics* **1998**, *17*, 2720–2729.

(40) Meiere, S. H.; Harman, W. D. *Organometallics* **2001**, *20*, 3876.



- 3: R = Me, R<sub>1</sub> = Me (1 : >20)  
 10: R = OMe, R<sub>1</sub> = OMe (1 : 1)  
 11: R = OMe, R<sub>1</sub> = H (2 : 1)  
 12: R = NMe<sub>2</sub>, R<sub>1</sub> = H (1 : <20)



- 13: R = TMS (1 : 1)  
 14: R = C(Me)(OCH<sub>2</sub>CH<sub>2</sub>O) (1 : 1)  
 15: R = C(CH<sub>3</sub>)<sub>3</sub> (A : B : C : D : 1 : 2 : 2 : 1)

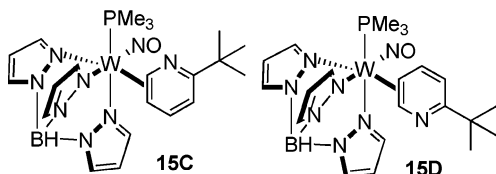


Figure 4. Stereo- and regiochemistry of pyridine complexes.<sup>40</sup>

Table 3. <sup>13</sup>C Data for 3, 10–15

|           | carbon resonance (ppm) |       |       |       |       |
|-----------|------------------------|-------|-------|-------|-------|
|           | a                      | b     | c     | d     | e     |
| class III |                        |       |       |       |       |
| 10B       | 174.8                  | 50.5  | 63.2  | 89.7  | 154.7 |
| 11B       | 170.0                  | 51.7  | 63.1  | 116.0 | 128.3 |
| 12B       | -                      | 49.5  | 60.7  | 259.5 | 128.2 |
| 14B       | 167.4                  | 60.0  | 64.9  | 119.3 | -     |
| 15B       | 166.2                  | 59.7  | 64.8  | 116.3 | -     |
| class II  |                        |       |       |       |       |
| 10A       | 171.4                  | 49.2  | 64.8  | 90.5  | 153.5 |
| 11A       | 173.5                  | 51.9  | 61.5  | 119.3 | 127.4 |
| class I   |                        |       |       |       |       |
| 15C       | -                      | 109.6 | 142.0 | 58.0  | 88.6  |

deprotonation of the protonated 2-acetylpyridine complex is immediately followed by decomposition to paramagnetic materials.

A single crystal of the  $\eta^2$ -pyridinium complex **16B** was isolated and a structural analysis by X-ray diffraction was carried out. An ORTEP of this structure appears in Figure 5, supporting the assignment of the **B** diastereomer. The pyridine ring shows significant distortions in C–C and C–N bond lengths that are consistent with a localization of electron density as depicted in Scheme 2. Compared to the structure of the neutral 2-(dimethylamino)pyridine complex **12**,<sup>41</sup> the C–C bond straddled by tungsten in **16B** is significantly longer (1.474(4) cf. 1.448(6) Å) indicating increased backbonding into the cationic ligand. Pioneering work by the Wigley<sup>39,42,43</sup> and Wolczanski<sup>15–17</sup> groups have established a rich chemistry of the d<sup>2</sup> metals Nb<sup>II</sup>

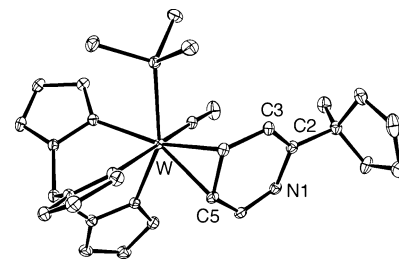
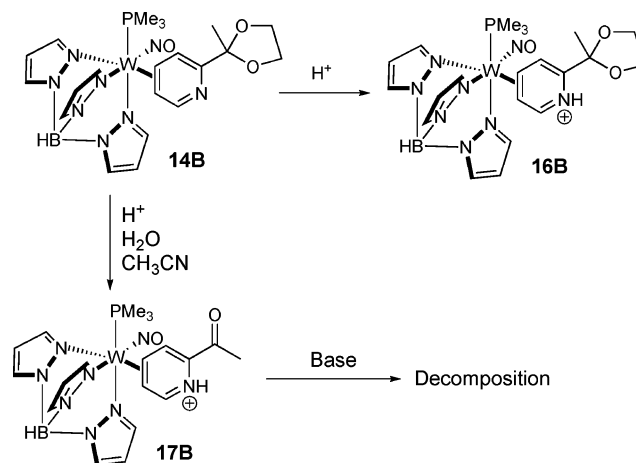


Figure 5. ORTEP of protonated  $\eta^2$ -pyridine complex **16B** (triflate salt). Selected bond lengths (Å) and angles (deg): W–C(4): 2.226(3); W–C(5): 2.239(3); N(1)–C(6): 1.315(4); C(6)–C(5): 1.393(4); C(5)–C(4): 1.474(4); C(4)–C(3): 1.460(4); C(3)–C(2): 1.332(4); N(1)–C(2): 1.404(5). O(3)–N(8)–W: 177.7(2).

Scheme 2. Protonation and Hydrolysis of 2-(2-Methyl-1,3-dioxolan-2-yl)pyridine Complex



and Ta<sup>III</sup> with pyridines. In contrast to the d<sup>6</sup> systems, the d<sup>2</sup> pyridine complexes, which also show extensive localization of the ring  $\pi$  system,<sup>17</sup> are exclusively bound across the C–N bond of the heterocycle. This is even the case when both the 2 and 6 positions are substituted (e.g., 2,6-lutidine,<sup>17</sup> NC<sub>5</sub><sup>t</sup>Bu<sub>3</sub>H<sub>2</sub><sup>39</sup>).

Key to the utility of these complexes in the stereoselective formation of isoquinuclidines is the ability to control the coordination diastereomer ratio (cdr). As with the lutidine complex, the ratio of isomers can be manipulated through taking advantage of solubility differences or converting the pyridine complexes to their conjugate acids. We have found that these  $\eta^2$ -pyridine complexes and their protonated analogues show significant differences in regio- and stereochemical binding preference and an account of this follows.

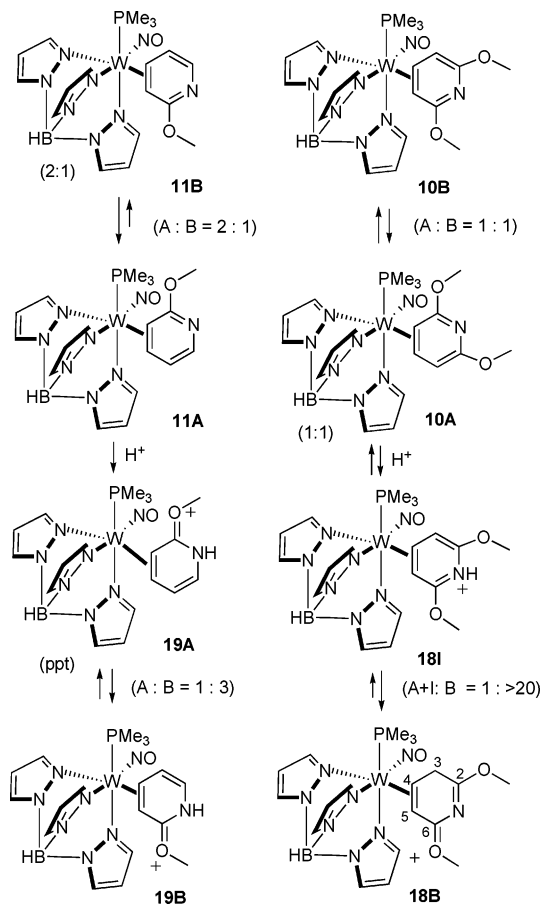
The dimethoxypyridine complex **10** exists as a 1:1 equilibrium mixture of two diastereomers **10A** and **10B**, while the 2-methoxypyridine complex **11** has an equilibrium ratio of 2:1 (**11A**:**11B**), with the major isomer having its methoxy group oriented toward the PMe<sub>3</sub>. Protonations of the methoxypyridine and dimethoxypyridine complexes initially occur at nitrogen. For example, complex **10** reacts with diphenylammonium triflate (DPhAT) in acetone to produce a species that is thought to be [TpW(NO)(PMe<sub>3</sub>)(3,4- $\eta^2$ -2,6-1*H*-dimethoxypyridinium)](OTf). This transient<sup>44</sup> (**18I**) is slowly replaced by a new complex **18**, identified as the 5*H*-pyridinium species (Scheme 3). This remarkable example of protonation of a pyridine carbon over nitrogen is first formed in a ratio of 2:1 (**18A**:**18B**). However, within 1 h the complete isomerization to coordination

(41) ORTEP diagram shown in Ref 20.

(42) Gray, S. D.; Smith, D. P.; Bruck, M. A.; Wigley, D. E. *J. Am. Chem. Soc.* **1992**, *114*, 5462–5469.

(43) Smith, D. P.; Strickler, J. R.; Gray, S. D.; Bruck, M. A.; Holmes, R. S.; Wigley, D. E. *Organometallics* **1992**, *11*, 1275–1278.

(44) identified by a unique set of Tp signals and a H3 doublet at 5.88 ppm.

**Scheme 3.** Stereochemistry of Protonation for Methoxy-substituted Pyridine Complexes (equilibrium ratios shown)

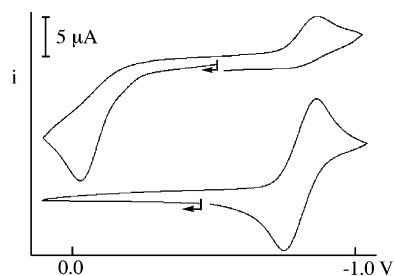
diastereoisomer **B** occurs ( $<1:20$ ), where the methoxy group is oriented away from the  $\text{PMe}_3$  (Scheme 3). Deprotonation of **18** with the base 1,8-diazabicyclo[5.4.0]undec-7-ene (DBU) returns complex **10** in a ratio of  $<1:20$  A:B, but within 45 min the solution of **10** re-equilibrates to a 1:1 ratio. Protonation of methoxypyridine **11** with pyridinium triflate results in a crystalline precipitate of  $[\text{TpW}(\text{NO})(\text{PMe}_3)(3,4\text{-}\eta^2\text{-}2\text{-}1H\text{-methoxypyridinium})](\text{OTf})$  (**19A**). Over a period of 48 h, a solution of **19A** equilibrates to its thermodynamic ratio of 1:3 (A:B) (see Scheme 3).

The 2-DMAP complex can be protonated with DPhAT at the pyridine nitrogen producing  $\text{TpW}(\text{NO})(\text{PMe}_3)(3,4\text{-}\eta^2\text{-}(2\text{-DMAP}))\cdot\text{HOTf}$  (**20**) in 65% yield and as a single diastereomer. Signals for the methyl groups, which are broadened in **12**, become sharp singlets, presumably because of an increased rotational barrier of the dimethylamino group. The trimethylsilylpyridine complex (**13**) protonates in DME with pyridinium triflate to produce  $\text{TpW}(\text{NO})(\text{PMe}_3)(4,5\text{-}\eta^2\text{-trimethylsilylpyridinium})\cdot\text{OTf}$  (**21**) and immediately precipitates from solution. The precipitate (**21**) exists as a single isomer, and subsequent deprotonation returns **13A**, exclusively as the A diastereomer. Over time the solution of **13A** reverts to its equilibrium mixture of 1:1 ( $t_{1/2} = 31$  min). The isomerization specific rate for this *interfacial* isomerization (face-flip) was measured to be  $3.7 \times 10^{-4} \text{ s}^{-1}$  at 23 °C. This corresponds to a free energy of activation of 21.9 kcal/mol. This barrier is consistent with previously reported  $\{\text{TpRe}(\text{CO})(\text{MeIm})\}$  complexes of heterocycles which have *interfacial* isomerization barriers of about 20 kcal/mol.<sup>34</sup>

**Table 4.** Summary of Kinetic and Thermodynamic Parameters for Tungsten Pyridine Complex (**2**)

| process                   | oxidation state | difference in free energy (kcal/mol) | free energy of activation (kcal/mol) |
|---------------------------|-----------------|--------------------------------------|--------------------------------------|
| W–N rotation              | W(0)            | 0                                    | 11                                   |
| N to 4,5 coordination     | W(0)            | 15 <sup>a</sup>                      | 37                                   |
| 4,5 to N coordination     | W(0)            | –15 <sup>a</sup>                     | 22                                   |
| intrafacial isomerization | W(0)            | 0                                    | 15–19 <sup>b</sup>                   |
| interfacial isomerization | W(0)            | 0                                    | 22 <sup>c</sup>                      |
| N to 4,5 coordination     | W(I)            | 33 <sup>a</sup>                      | $>33^a$                              |

<sup>a</sup> Based all or in part on DFT calculations. <sup>b</sup> Estimated from lutidine complex **3**. <sup>c</sup> Estimated from TMS pyridine complex **13**.

**Figure 6.** Cyclic voltammograms of  $\eta^2$ -2,6-lutidine (top) and pyridine ( $\kappa\text{N}$ ) complexes recorded at 100 mV/s.

Given that this rate is significantly slower than that for the interconversion of coordination diastereomers seen with 2,6-lutidine (*vide supra*), we assign the latter to an *intrafacial* isomerization (ring-walk).<sup>34</sup>

**Tungsten(I) Pyridine Complexes.** Tungsten(I) complexes are most conveniently prepared by the one-electron oxidation of their W(0) counterparts (Table 4). Our expectation was that the  $d^5$  complexes would not be sufficiently electron-rich to maintain  $\eta^2$ -coordination, and electrochemical experiments have borne this out. In Figure 6, a cyclic voltammogram is shown for both the 4,5- $\eta^2$ -2,6-lutidine complex (**3**) and the parent N-bound pyridine complex **2**. The N-bound pyridine complex shows a chemically reversible couple at  $-0.78$  V. In contrast, after electrochemical oxidation ( $E_{\text{pa}} = -0.07$  V) the  $\eta^2$ -lutidine complex (top) shows a reverse (i.e., negative) scan with a cathodic wave at  $E_{\text{pc}} = -0.85$  V at 50 mV/s, indicating a  $\eta^2$ -to-N linkage isomerization. This feature is observed even in the irreversibly binding solvent acetone,<sup>33</sup> and so we consider this linkage isomerization to be intramolecular in nature. Similar intramolecular  $\pi$ -to- $\sigma$  redox-coupled linkage isomerizations have been documented for pentaammineosmium(II)  $\pi$  complexes.<sup>45,46</sup> An additional feature in the cyclic voltammogram of lutidine complex **3** is the chemically irreversible nature of the oxidation of W(I)–pyridine species. This indicates that the linkage isomerization for 2,6-lutidine from N to  $\eta^2$  occurs with a limiting half-life of a few seconds at 22 °C.<sup>47</sup>

Finally, we hoped to gain insight into the kinetics of the N-to- $\eta^2$  isomerization and its reverse for the parent pyridine complex (**2**) by attempting to trap out the  $\eta^2$ -form with acid.<sup>48</sup> A DME solution of the pyridine complex **2** was treated with the weak acid pyHOTf and was allowed to stand for 1 h over which time

(45) Harman, W. D.; Taube, H. *J. Am. Chem. Soc.* **1988**, *110*, 5403–5407.(46) Harman, W. D.; Sekine, M.; Taube, H. *J. Am. Chem. Soc.* **1988**, *110*, 2439–2445.(47) Bard, A. J.; Faulkner, L. R. *Electrochemical Methods Fundamentals and Applications*; John Wiley & Sons: New York, 1980.(48) A similar event was observed with a N-bound pyrimidine complex in which a cycloaddition takes place with the purported minor  $\eta^2$  isomer. *Organometallics* **2006**, *25*, 5852–5853.

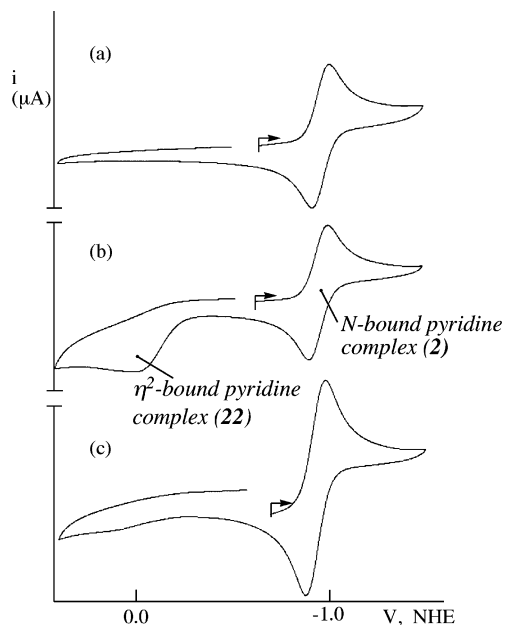


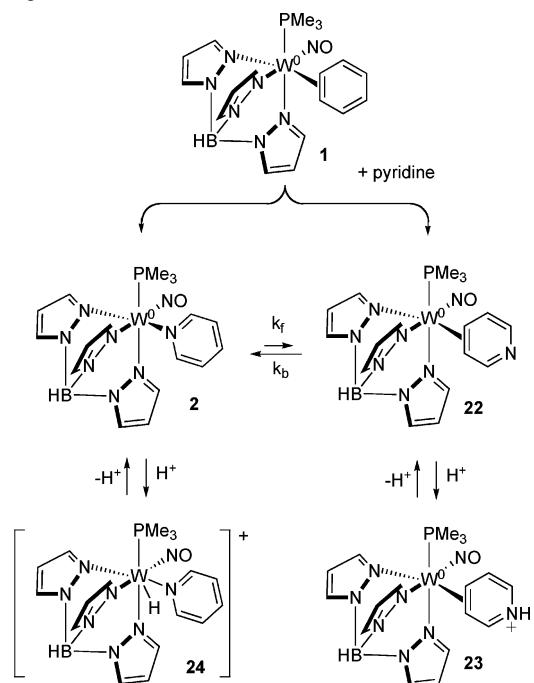
**Figure 7.** Cyclic voltammograms showing the isomerization of the  $\eta^2$ -pyridine **22**, to the N-bound isomer **2**. CVs recorded before (a), immediately after (b), and 3 h after (c) the deprotonation of pyridinium complex **23**.

a new compound (**24**) precipitated from solution. A  $^1\text{H}$  NMR spectrum showed a strong hydride signal at  $\delta$  12.42 split by  $^{31}\text{P}$  (121 Hz), as well as other peaks that indicate the presence of  $\text{PMe}_3$  a nitrogen-bound pyridine ligand, and Tp. These observations along with IR and CV data indicating a W(II) species lead us to the assignment of **24** as  $\text{TpW}(\text{NO})(\text{PMe}_3)(\text{py})(\text{H})$ .

Competitive binding studies show similar rates of binding for  $\{\text{TpW}(\text{NO})(\text{PMe}_3)\}$  pyridines and aromatic hydrocarbons, and we envisioned trapping a transient  $\eta^2$ -pyridine species via its protonation by a weak Brønsted acid. Thus, the benzene complex **1** was added to a pyridine solution that contained  $\text{py}\cdot\text{HOTf}$ , and after 5 h the reaction mixture was treated with hexanes to form an oil, which was partially manipulated into a bright orange solid (**23**, 14%). Compound **23** showed a  $^{31}\text{P}$  signal at  $-12.45$  ppm with a  $J_{\text{WP}}$  of 294 Hz. These values along with IR and CV data are similar to those observed for the  $\eta^2$  pyridinium complexes **4** and **16–19** (e.g., for the lutidinium complex **4**,  $\delta = -11.25$  and  $J_{\text{WP}} = 296$  Hz).<sup>41</sup> Proton and carbon NMR spectra of **23** indicated two diastereomers of  $\text{TpW}(\text{NO})(\text{PMe}_3)(\eta^2\text{-pyridinium})$  triflate (**23A**; 1:1 ratio of A to B). Over several hours, the ratio of **23A** to **23B** changed from 1:1 to 4:1 in acetone- $d_6$ . At this point, an excess of NaH was added to this solution causing the solution to change color from orange to dark blue-green. The resulting spectrum showed the presence of the elusive parent  $\eta^2$ -pyridine **22** as well as its N-bound isomer **2**. Judging from data in Table 2, the pyridine complex **22**, is formed as a 4:1 ratio of 4,5- $\eta^2$  isomers, presumably reflecting the isomer ratio of its precursor **23**. Additional minor proton peaks and a phosphorus signal at  $\delta -14.36$  suggested a second diastereomer, which also appeared to decay over time, but the COSY data was not of sufficient quality to determine the nature of this second isomer of **22**.

A cyclic voltammogram of **22** shows an anodic wave at  $E_{\text{p,a}} = 0.00$  V, which on return scan leads to an increase in the N-bound pyridine couple  $-0.78$  V (Figure 7). Over time, a series of first scans indicates that **22** decreases with a half-life of 79

**Scheme 4**  $\eta^2/\text{N}$  Isomerization for Pyridine Complex **2** and the Trapping of Minor Isomer **25** with Acid



min, while the N-bound isomer **2** ( $E_{1/2} = -0.78$  V) increases by the corresponding amount. Taken together, these observations indicate the relationship between **2**, **22**, and **23** as outlined in Scheme 4. The  $\eta^2 \rightarrow \text{N}$  isomerization (i.e., **22**  $\rightarrow$  **2**) occurs for pyridine with a  $k_b = 1.5 \times 10^{-4} \text{ s}^{-1}$  at 22 °C. In consideration of the calculated  $\Delta E$  for the N to  $\eta^2$  isomerization (14.9 kcal/mol), we can estimate a specific rate for the N to  $\eta^2$  isomerization for the pyridine complex **2** of  $k_f = 1.4 \times 10^{-15} \text{ s}^{-1}$  at 22 °C. Thus, it becomes clear that our attempts to trap the  $\eta^2$ -pyridine starting from the N-bound isomer were futile. However, the slower than expected rate for conversion of the  $\eta^2$ -isomer **22** to the N-bound form allows its capture immediately after complexation. Finally, if one assumes that the value of  $E_{\text{p,a}}$  is similar to  $E^\circ$  for the  $\eta^2$ -pyridine complex **22**,<sup>45</sup> and the N to  $\eta^2$  isomerization energy for **2** is taken as 14.9 kcal/mol, a thermodynamic cycle can be derived that provides an estimate for the N to  $\eta^2$  isomerization for W(I) of 33 kcal/mol.

It is worth noting that the observed rate of  $k_b = 1.5 \times 10^{-4} \text{ s}^{-1}$  for the  $\eta^2 \rightarrow \text{N}$  isomerization reflects the conversion from the class III (C4,C5- $\eta^2$ ) isomer and does not necessarily reflect the isomerization barrier from a C,N- $\eta^2$  isomer (class V or VI). It is possible that the rate-determining step is actually an intrafacial isomerization to class V or VI prior to the conversion to the N-bound isomer **2**.

## Conclusion

The ability of tungsten to bind pyridines in an  $\eta^2$  manner is dependent on both the electronic and steric properties of the substituents as well as the oxidation state of the metal. Although DFT calculations suggest there to be about 15 kcal difference in energy between the N- and  $\eta^2$ -bound forms for the W(0) pyridine complex (**2**), a single bulky substituent at C2 can discourage the metal from binding through the nitrogen. Electron-releasing substituents at C2 also cause coordination at the C4–C5 position. This arrangement allows for an



interaction of the  $\pi$  substituent with the 2-azadiene-like uncoordinated fragment, providing stability for this isomer, relative to either N-bound or C–H activated isomers. In contrast, the weaker  $\pi$  acid W(I) binds pyridines at N only, owing to an insurmountable difference in binding energies.

In the majority of cases in which  $\eta^2$ -binding is favorable, the metal binds across the C4–C5 position exposing an uncoordinated  $\pi$ -system that resembles a 2-azadiene. Given that 2-azadienes are more reactive toward cycloaddition reactions than their 1-azadiene counterparts,<sup>49</sup> and that differences in energies between N- and  $\eta^2$ -bonding modes is modest for W(0), the complex {TpW(NO)(PMe<sub>3</sub>)} holds real promise as an agent that can activate pyridines toward cycloaddition reactions,<sup>41</sup> even if the N-bound isomer of the pyridine complex is thermodynamically favored.

## Experimental Section

**General Methods.** NMR spectra were obtained on a 300 or 500 MHz Varian INOVA or a 300 or 500 MHz Avance Bruker spectrometer. All chemical shifts are reported in ppm and are referenced to tetramethylsilane (TMS) utilizing residual <sup>1</sup>H or <sup>13</sup>C signals of the deuterated solvents as an internal standard. Coupling constants (*J*) are reported in hertz (Hz). Resonances in the <sup>1</sup>H NMR due to pyrazole ligands (Tp) are listed by chemical shift and multiplicity only (all coupling constants are 2 Hz). Infrared spectra (IR) were recorded on a MIDAC Prospect Series (Model PRS) spectrometer as a glaze on a horizontal attenuated total reflectance (HATR) accessory (Pike Industries). Electrochemical experiments were performed under a dinitrogen atmosphere using a BAS Epsilon EC-2000 potentiostat. Cyclic voltammetry data was taken at ambient temperature at 100 mV/s (25 °C) (unless otherwise specified) in a standard three-electrode cell from +1.7 to –1.7 V with a glassy carbon working electrode, *N,N*-dimethylacetamide (DMA) solvent, and tetrabutylammonium hexafluorophosphate (TBAH) electrolyte (~0.5 M). All potentials are reported versus NHE (normal hydrogen electrode) using cobaltocenium hexafluorophosphate ( $E_{1/2} = -0.78$  V) or ferrocene ( $E_{1/2} = 0.55$  V) as an internal standard. The peak-to-peak separation was less than 100 mV for all reversible couples. Mass spectra were obtained on either a JEOL JMS600 using FAB<sup>+</sup>, or a Finnigan MAT TSQ7000 using ESI<sup>+</sup>; no counter ions were observed. Unless otherwise noted, all synthetic reactions and electrochemical experiments were performed under a dry nitrogen atmosphere. CH<sub>2</sub>Cl<sub>2</sub>, benzene, THF (tetrahydrofuran), and hexanes were purged with nitrogen. Other solvents and liquid reagents were thoroughly purged with nitrogen prior to use. Lutidine was distilled before use. Pyridinium triflate was synthesized by adding triflic acid to pyridine. Deuterated solvents were used as received from Cambridge Isotopes. Synthesis and characterization of compounds **1**,<sup>20</sup> **3**, **4**, **12**, and **20** have been previously published.<sup>21</sup>

**TpW(NO)(PMe<sub>3</sub>)(pyridine) (2).** A solution of pyridine (0.90 g) in 1,2-dimethoxyethane (DME) (7 mL) was prepared and passed through activated alumina into a screwcap vial charged with a stirbar and TpW(NO)(PMe<sub>3</sub>)( $\eta^2$ -benzene) (493 mg, 0.85 mmol). The vial was capped, and the solution allowed to stir for 4.5 h at which time the dark turquoise reaction mixture was added slowly to 100 mL of stirring pentane. The resulting suspension was reduced to 75 mL under reduced pressure and the precipitate collected on a medium porosity 30 mL frit. The precipitate was dried *in vacuo* to yield **2** (300 mg, 0.51 mmol, 60% yield) as a dark turquoise powder. IR (HATR glaze):  $\nu_{\text{NO}} = 1503\text{cm}^{-1}$ . CV:  $E_{1/2} = -0.78$  V. <sup>1</sup>H NMR (acetone-*d*<sub>6</sub>,  $\delta$ ): 7.92 (1H, d (*J* = 1.8), Tp 3 or 5), 7.87 (1H, d (*J* = 2.4), Tp 3 or 5), 7.81 (1H, d (*J* = 2.1), Tp 3 or 5), 7.75 (1H, br s, Tp 3 or 5), 7.6 (very br s, py 2, 6), 7.51

(1H, d (*J* = 1.8), Tp 3 or 5), 7.23 (1H, d (*J* = 1.5), Tp 3 or 5), 6.57 (2H, t (*J* = 7.2), py 3, 5), 6.34 (1H, t (*J* = 2.4), Tp 4), 6.26 (1H, t (*J* = 2.4), Tp 4), 6.26 (1H, t (*J* = 2.4), Tp 4), 5.97 (1H, br t (*J* = 6.9), py 4), 1.41 (9H, d (*J* = 7.2), PMe<sub>3</sub>). <sup>13</sup>C NMR (dimethylformamide-*d*<sub>7</sub>,  $\delta$ ): 143.1 (s, Tp 3 or 5), 140.3 (s(br), Tp 3 or 5), 135.9 (s, Tp 3 or 5), 135.7 (s(br), Tp 3 or 5), 135.5 (s, Tp 3 or 5), 106.5 (s, Tp 4), 106.1 (s, Tp 4), 106.0 (s, Tp 4), 124.9 (s(br), py 4), 121.6 (s(br) py 3 and 5).

**TpW(NO)(PMe<sub>3</sub>)(3,4- $\eta^2$ -2,6-Dimethoxypyridine) (1:1) (10).** To a solution of TpW(NO)(PMe<sub>3</sub>)( $\eta^2$ -benzene) (1.01 g, 1.74 mmol) and 2,6-dimethoxypyridine (3.77 g, 27.1 mmol, 16 equiv) was added pentane (6 mL). The resulting heterogeneous mixture was stirred for 26 h. The reaction mixture was then added to 50 mL pentane, and the resulting precipitate was collected on a medium porosity frit and dried *in vacuo* to give **10** (885.4 mg, 1.379 mmol, 79%) as a tan powder. IR (HATR glaze):  $\nu_{\text{NO}} = 1567\text{cm}^{-1}$ . CV:  $E_{\text{p,a}} = -0.18$  V. HRMS (*m/z*, obs(I); calc(I); error): 640.16889 (20%); 640.17061 (18%); –2.7 ppm, 641.16742 (92%); 641.16793 (86%); –0.8 ppm, 642.1705 (81%); 642.17049 (79%); 0.0 ppm, 643.17073 (100%); 643.17029 (100%); 0.7 ppm, 644.1737 (44%); 644.17456 (41%); –1.3 ppm, 645.17361 (81%); 645.17355 (85%); 0.1 ppm, 646.17585 (19%); 646.17599 (19%) –0.2 ppm. <sup>1</sup>H NMR (acetone-*d*<sub>6</sub>,  $\delta$ ) (1:1 isomer ratio): 8.32 (1H, br s, Tp), 8.16 (1H, br s, Tp), 8.00 (1H, br s, Tp), 7.96 (3H, br s, 3 Tp), 7.95 (1H, br s, Tp), 7.92 (1H, br s, Tp), 7.84 (1H, br s, Tp), 7.77 (1H, br s, Tp), 7.46 (1H, br s, Tp), 7.39 (1H, br s, Tp), 6.37 (1H, br s, Tp), 6.35 (1H, br s, Tp), 6.30 (2H, br s, 2 Tp), 6.29 (1H, bs, Tp), 6.23 (1H, bs, Tp), 5.45 (1H, d (*J* = 5.8), 5A), 5.22 (1H, d (*J* = 4.6), 5B), 4.17 (1H, ddd (*J* = 4.6, 10.0, 14.3), 4B), 3.86 (3H, s, 7 or 8 (A or B)), 3.83 (3H, s, 7 or 8 (A or B)), 3.67 (1H, dd (*J* = 2.3, 9.9), 3A), 3.65 (3H, s, 7 or 8 (A or B)), 3.61 (3H, s, 7 or 8 (A or B)), 2.23 (1H, ddd (*J* = 2.3, 5.8, 7.3), 4A), 2.08 (1H, d (*J* = 10.0), 3B), 1.78 (18H, d (*J* = 8.6), PMe<sub>3</sub> (A+B)). <sup>13</sup>C NMR (acetone-*d*<sub>6</sub>,  $\delta$ ): 174.8 (s, 2B), 171.4 (s, 2A), 154.7 (s, 6B), 153.5 (s, 6A), 145.6 (s, Tp), 145.1 (s, Tp), 144.7 (s, Tp), 141.7 (s, 2 Tp), 141.5 (s, Tp), 137.7 (s, Tp), 137.6 (s, Tp), 137.0 (s, 2 Tp), 136.6 (s, Tp), 136.4 (s, Tp), 107.3 (s, Tp), 107.2 (s, Tp), 107.0 (s, 2 Tp), 106.2 (s, Tp), 105.8 (s, Tp), 90.5 (s, 5A), 89.7 (d (*J* = 3.4), 5B), 64.8 (d (*J* = 10.3), 4B), 63.2 (s, 4A), 55.0 (s, 7A or 7B (MeO)), 54.9 (s, 7A or 7B (MeO)), 52.5 (s, 8A or 8B (MeO)), 52.3 (s, 8A or 8B (MeO)), 50.5 (s, 3B), 49.2 (d (*J* = 8.0), 3A), 13.7 (d (*J* = 27.6), PMe<sub>3</sub> A or B), 13.0 (d (*J* = 28.2), PMe<sub>3</sub> A or B), <sup>31</sup>P: (acetone-*d*<sub>6</sub>,  $\delta$ ): –14.11 (satellite d (*J* = 299), PMe<sub>3</sub>), –11.72 (satellite d (*J* = 310), PMe<sub>3</sub>).

**TpW(NO)(PMe<sub>3</sub>)(3,4- $\eta^2$ -2-Methoxypyridine) (2:1) (11).** To a solution of TpW(NO)(PMe<sub>3</sub>)( $\eta^2$ -benzene) (1.01 g, 1.74 mmol) and 2-methoxypyridine (2.70 g, 24.7 mmol, 12 equiv) was added pentane (6 mL). The resulting heterogeneous mixture was stirred for 48 h. The reaction mixture was then added to pentane (50 mL), and the resulting precipitate was collected on a medium porosity frit, washed with 1:1 pentane:diethyl ether (30 mL), and then dried *in vacuo* to give **11** (1.01 g, 1.65 mmol, 79%) as a yellow powder. IR (HATR glaze):  $\nu_{\text{NO}} = 1571\text{cm}^{-1}$ . CV:  $E_{\text{p,a}} = 0.06$  V. MS (ESI<sup>+</sup>): *m/z* = 612 [M]<sup>+</sup>. HRMS (*m/z*, obs(I); calc(I); error): 610.15276 (34%); 610.16004 (18%); –11.9 ppm, 611.15556 (98%); 611.15735 (86%); –2.9 ppm, 612.15755 (91%); 612.15991 (79%); –3.9 ppm, 613.15956 (100%); 613.15968 (100%); –0.2 ppm, 614.16076 (55%); 614.16402 (40%); –5.3 ppm, 615.16283 (86%); 615.16295 (85%); –0.2 ppm, 616.16384 (18%); 616.16536 (19%); –2.5 ppm. <sup>1</sup>H NMR (CDCl<sub>3</sub>,  $\delta$ ) (2:1 isomer ratio): 8.23 (1H, br s, Tp A), 8.11 (1H, br s, Tp B), 7.95 (1H, br s, Tp B), 7.92 (1H, br s, Tp A), 7.75 (3H, br s, 2 Tp A + Tp B), 7.72 (1H, br s, Tp B), 7.64 (1H, br s, Tp A), 7.60 (1H, br s, Tp B), 7.14 (1H, br s, Tp B), 7.11 (1H, br s, Tp A), 6.42 (1H, d (*J* = 6.1), 5A), 6.41 (1H, buried, 6A), 6.39 (1H, d (*J* = 6.1), 6B), 6.25 (2H, br s, Tp A + Tp B), 6.20 (4H, br s, 2 Tp A + 2 Tp B), 6.02 (1H, dd (*J* = 4.8, 6.1), 5B), 3.98 (1H, buried, 4B), 3.91 (3H, s, 7A), 3.90 (3H, s, 7B), 3.62 (1H, dd (10.2, 12.0), 3A), 2.26 (2H, buried, 3B + 4A), 1.26 (9H, d (*J* = 8.3), PMe<sub>3</sub> A), 1.23 (9H, d (*J* = 8.3), PMe<sub>3</sub> B). <sup>13</sup>C NMR (CDCl<sub>3</sub>,  $\delta$ ): 173.5 (s, 2B), 170.0 (s, 2A), 144.9 (s, Tp B), 144.3 (s, Tp B), 144.2 (s, Tp A),

(49) Ghosez, L.; Bayard, P.; Nshimyumukiza, P.; Gouvernuer, V.; Sainte, F.; Beaudegnies, R.; Rivera, M.; Frisque-Hesbain, A. M.; Wynants, C. *Tetrahedron* **1995**, *51*, 11021–11042.

142.0 (s, Tp A), 140.2 (s, Tp A), 140.1 (s, Tp B), 136.7 (s, Tp B), 136.6 (s, Tp A), 136.2 (s, Tp B), 136.1 (s, Tp A), 135.6 (s, Tp B), 135.5 (s, Tp A), 128.3 (s, 6B), 127.4 (s, 6A), 119.3 (s, 5A), 116.0 (s, 5B), 106.6 (s, Tp B), 106.5 (s, Tp A), 106.2 (s, Tp B), 106.1 (s, Tp A), 105.6 (s, Tp A), 105.2 (s, Tp B), 63.1 (d ( $J = 9.2$ ), 4B), 61.5 (s, 4A), 52.5 (s, 7B), 52.2 (s, 7A), 51.9 (s, 3A), 51.7 (d ( $J = 7.6$ ), 3B), 13.8 (d ( $J = 27.5$ ),  $\text{PMe}_3$  A), 13.2 (d ( $J = 27.5$ ),  $\text{PMe}_3$  B).  $^{31}\text{P}$  NMR: (acetone- $d_6$ ,  $\delta$ ):  $-12.71$  (satellite d ( $J = 300$ ),  $\text{PMe}_3$  A),  $-11.66$  (satellite d ( $J = 298$ ),  $\text{PMe}_3$  B).

**TpW(NO)(PMe)<sub>3</sub>( $\eta^2$ -4,5- $\eta^2$ -2-Trimethylsilylpyridine) (1:1) (13).** 2-Trimethylsilylpyridine (0.5 mL) was added to a solution of **1** (142.3 mg, 0.245 mmol) in THF (1 mL). After 3h, the reaction mixture was added to pentane (50 mL) and the resulting precipitate was collected on a medium porosity glass filter and dried *in vacuo* to give **13** (81.8 mg, 0.125 mmol, 51%) as a yellow powder. This compound is substitution labile and was carried on to **21** without purification. IR (HATR glaze):  $\nu_{\text{NO}} = 1579 \text{ cm}^{-1}$ . CV:  $E_{\text{pa}} = +0.03 \text{ V}$ .  $^1\text{H}$  NMR (acetone- $d_6$ ,  $\delta$ ): 8.55 (1H, d ( $J = 3.4$ ), 6A), 8.39 (1H, br s, 6B), 8.19 (2H, d, 2 Tp), 7.99 (4H, br s, 4 Tp), 7.97 (2H, d, 2 Tp), 7.86 (1H, d, Tp), 7.84 (1H, d, Tp), 7.48 (1H, d, Tp), 7.43 (1H, d, Tp), 6.95 (1H, d ( $J = 5.2$ ), 3B), 6.71 (1H, d ( $J = 4.9$ ), 3A), 6.37 (2H, t, 2 Tp), 6.34 (2H, t, 2 Tp), 6.31 (2H, t, 2 Tp), 3.88 (2H, m, 4B + 5A), 2.2 (1H, br s, 5B), 2.16 (1H, d ( $J = 8.2$ ), 4A), 1.33 (9H, d ( $J = 8.2$ ),  $\text{PMe}_3$  B), 1.30 (9H, d ( $J = 8.5$ ),  $\text{PMe}_3$  A), 0.18 (9H, s, TMS B), 0.16 (9H, s, TMS A).  $^{31}\text{P}$  NMR: (acetone- $d_6$ ,  $\delta$ ):  $-12.13$  (satellite d ( $J = 302$ ),  $\text{PMe}_3$  A),  $-14.96$  (satellite d ( $J = 293$ ),  $\text{PMe}_3$  B).

**TpW(NO)(PMe)<sub>3</sub>( $\eta^2$ -4,5-(2-(2-Methyl- $^{13}\text{C}$ -dioxolan-2-yl)pyridine)) (14B).** TpW(NO)(PMe)<sub>3</sub>( $\eta^2$ -benzene) (100 mg) was dissolved in minimal 2-(2-methyl- $^{13}\text{C}$ -dioxolan-2-yl)pyridine then added diethyl ether (3 mL) and stirred for 18 h. More diethyl ether (10 mL) was added, and the precipitate was collected on a fine porosity frit and washed with diethyl ether (10 mL). Isolated compound **14B** (72 mg, 63% yield) as a yellow solid. IR:  $\nu_{\text{NO}} = 1576 \text{ cm}^{-1}$ . CV:  $E_{\text{pc}} = 0.07 \text{ V}$ ,  $E_{\text{pa}} = 0.99 \text{ V}$ . HRMS ( $m/z$ , obs(I); calc(I); error): 666.18734 (18%); 666.18626 (18%); 1.6 ppm, 667.18502 (87%); 667.18361 (85%); 2.1 ppm, 668.1876 (80%); 668.18616 (80%); 2.2 ppm, 669.18634 (100%); 669.18600 (100%); 0.5 ppm, 670.19101 (41%); 670.19017 (43%); 1.3 ppm, 671.19081 (83%); 671.18924 (84%); 2.3 ppm, 672.19309 (21%); 672.19172 (21%); 2.0 ppm.  $^1\text{H}$  NMR (chloroform- $d$ ):  $\delta$  8.77 (1H, d,  $J = 3.7 \text{ Hz}$ , 6), 8.30 (1H, d,  $J = 1.5 \text{ Hz}$ , Tp), 7.90 (1H, d,  $J = 1.8 \text{ Hz}$ , Tp), 7.76 (2H, d,  $J = 2.4 \text{ Hz}$ , Tp), 7.64 (1H, d,  $J = 1.8 \text{ Hz}$ , Tp), 7.12 (1H, d,  $J = 1.5 \text{ Hz}$ , Tp), 6.70 (1H, d,  $J = 5.5 \text{ Hz}$ , 3), 6.27 (2H, t,  $J = 1.5$ , 2.5 Hz, Tp 4), 6.21 (1H, t,  $J = 1.83$ , 2.5 Hz, Tp 4), 4.13 (1H, m, CH<sub>2</sub>), 3.98 (3H, m, CH<sub>2</sub>), 3.79 (1H, ddd,  $J = 5.5$ , 9.1, 13.7 Hz, 4), 2.32 (1H, d,  $J = 3.6$ , 9.5, 5), 1.81 (3H, s, Me), 1.29 (9H, d,  $J = 8.24$ ,  $\text{PMe}_3$ ).  $^{13}\text{C}$  NMR (chloroform- $d$ ):  $\delta$  167.4 (s, 6), 144.1 (s, Tp), 144.0 (s, Tp), 140.0 (s, Tp), 136.7 (s, Tp), 136.4 (s, Tp), 135.3 (s, Tp), 119.3 (s, 3), 106.5 (s, Tp 4), 106.2 (s, Tp 4), 106.1 (s, Tp 4), 64.9 (s, 4), 64.7 (s, CH<sub>2</sub>), 64.3 (s, CH<sub>2</sub>), 60.0 (s, 5), 27.0 (s, CH<sub>3</sub>), 13.2 (d,  $J = 28.3$ ,  $\text{PMe}_3$ ).

**TpW(NO)(PMe)<sub>3</sub>( $\eta^2$ -(2-tertbutylpyridine)) (15).** Compound **1** (140 mg) was dissolved with 2-tertbutylpyridine (0.3 mL), pentane (2 mL), and diethyl ether (1 mL) and stirred for 18 h. The product was precipitated into pentane (75 mL) and was collected on a fine porosity frit. The product was then washed with pentane (15 mL) and dried *in vacuo*. Isolated compound **15** (65 mg 42% yield) as a mixture of four isomers. This complex is not stable in solution over extended periods of time and could not be purified, but partial assignments of proton resonances could be made using COSY data. CV:  $E_{1/2} = -0.10 \text{ V}$ .  $^1\text{H}$  NMR (selected resonances, acetone- $d_6$ ): ( $\delta$ ) 8.63 (1, d,  $J = 3.7$ , 6B), 8.42 (d, 6A) 7.5 (1, m (buried), 4C), 7.4 (dd, buried, 4D), 6.5(d, 3A) 6.4 (6, buried, 3B), 5.85 (d,  $J = 9.0$ , 3D) 5.82 (1, d,  $J = 9.3$ , 3C), 5.73 (1, ddd,  $J = 1.1$ , 7.6, 14.0, 6C), 4.20 (br d,  $J = 8$ , 6D), 4.00 (1, dddd,  $J = 1.1$ , 5.80, 13.9, 15.3, 4B), 3.82 (m, 5A) 3.62 (m, 5D) 2.21 (1, m, 5B), 2.07 (1, m, 5C).  $^{13}\text{C}$  NMR (selected resonances, acetone- $d_6$ ):  $\delta$  166.2 (s, 6B), 142.0 (s, 4C), 116.3 (s, 3B), 109.6 (s, 3C), 88.6 (s, 6C),

64.8 (s, 4B), 59.7 (s, 5B), 58.0 (s, 5C), 31.2 (s, 'Bu), 30.5 (s, 'Bu), 13.5 (d,  $J = 19.9 \text{ Hz}$ ,  $\text{PMe}_3$ ), 13.1 (d,  $J = 20.2 \text{ Hz}$ ,  $\text{PMe}_3$ ).

**TpW(NO)(PMe)<sub>3</sub>( $\eta^2$ -4,5-(2-(2-Methyl- $^{13}\text{C}$ -dioxolan-2-yl)-pyridinium)) (16).** Compound **14** (75 mg) was dissolved in acetone (1 mL), PyHOTf (28 mg) was added and stirred for 5 min. The product was precipitated in diethyl ether (30 mL) and collected over a fine porosity frit and dried *in vacuo*. Compound **16** was collected (66 mg, 72% yield) as a red solid.  $^1\text{H}$  NMR (acetonitrile- $d_3$ ):  $\delta$  8.66 (1, d,  $J = 6.4 \text{ Hz}$ , 6), 7.99 (3, d,  $J = 2.4 \text{ Hz}$ , Tp), 7.93 (1, d,  $J = 1.7$ , Tp), 7.84 (1, d,  $J = 2.3$ , Tp), 7.47 (1, d,  $J = 1.9$ , Tp), 6.89 (1, d,  $J = 5.6$ , 3), 6.42 (1, t,  $J = 2.2$ , Tp4), 6.39 (2, t,  $J = 2.3$ , Tp4), 4.01 (4, m, CH<sub>2</sub>,CH<sub>2</sub>), 3.86 (1, ddd,  $J = 5.65$ , 5.65, 11.7, 4), 2.43 (1, t,  $J = 6.41$ , 6.8, 5), 1.70 (3, s, Me), 1.23 (9, d,  $J = 9.0$ ,  $\text{PMe}_3$ ).  $^{13}\text{C}$  NMR (acetonitrile- $d_3$ ):  $\delta$  145.0 (s, 6), 144.9 (s, Tp), 144.5 (s, Tp), 141.2 (s, Tp), 137.9 (s, Tp), 137.4 (s, Tp), 136.6 (s, Tp), 129.7 (s, 2), 123.3 (s, 3), 107.1 (s, Tp), 106.7 (s, Tp), 106.6 (s, Tp), 104.6 (s, 7), 65.0 (s, 4), 64.8 (s, CH<sub>2</sub>), 64.6 (s, CH<sub>2</sub>), 57.7 (s, 5), 26.2 (s, Me), 11.6 (d,  $J = 30.9 \text{ Hz}$ ,  $\text{PMe}_3$ ).

**TpW(NO)(PMe)<sub>3</sub>( $\eta^2$ -1-Pyridinium-2-yl-ethanone) (17).** Compound **21** (105 mg) was dissolved in acetonitrile (2 mL) then water (8 drops) and HOTf (45 mg) were added. The reaction was stirred for 10 min. The solution was then slowly added to diethyl ether (75 mL) and the precipitate was collected on a fine porosity frit and dried *in vacuo*. Compound **17** was obtained (88 mg, 76% yield) as a light brown solid.  $^1\text{H}$  NMR (acetonitrile- $d_3$ ):  $\delta$  10.50 (1, s(br), NH), 8.75 (1, dd,  $J = 5.19$ , 7.78 Hz, 6), 8.05 (1, d,  $J = 2.4$ , Tp), 8.03 (1, d,  $J = 2.4$ , Tp), 8.01 (1, d,  $J = 2.4$ , Tp), 7.87 (3, m, 3, Tp), 7.57 (1, d,  $J = 2.2$ , Tp), 6.45 (2, dt,  $J = 2.3$ , Tp 4, Tp 4), 6.40 (1, t,  $J = 2.3$ , Tp 4), 3.89 (1, ddd,  $J = 0.92$ , 5.95, 11.6, 4), 2.56 (1, t,  $J = 5.3$ , 5), 2.48 (3, s, Me), 1.26 (9, d,  $J = 9.1 \text{ Hz}$ ,  $\text{PMe}_3$ ).  $^{13}\text{C}$  NMR (acetonitrile- $d_3$ ):  $\delta$  189.8 (s, CO), 171.4 (s, 6), 146.2 (s, Tp), 145.7 (s, Tp), 142.6 (s, Tp), 139.2 (s, Tp), 138.9 (s, Tp), 138.3 (d,  $J = 3.4 \text{ Hz}$ , 3), 138.0 (s, Tp), 108.5 (s, Tp 4), 108.1 (s, Tp 4), 107.9 (s, Tp 4), 65.5 (d,  $J = 10.5$ , 4), 58.9 (s, 5), 24.2 (s, Me), 12.8 (d,  $J = 31.3$ ,  $\text{PMe}_3$ ).

**TpW(NO)(PMe)<sub>3</sub>(3,4- $\eta^2$ -2,6-Dimethoxyppyridinium)(OTf) (2:1 A:B kinetic)(thermo <1:20) (18):** TpW(NO)(PMe)<sub>3</sub>(3,4- $\eta^2$ -2,6-Dimethoxyppyridine) (81.5 mg, 0.127 mmol) was dissolved in acetone (1 mL). DPhAT (46.5 mg, 0.146 mmol 1.1 equiv) dissolved in acetone (1 mL) was added after 45 min. The reaction was then added to diethyl ether (50 mL) and the resulting precipitate was collected on a medium porosity frit and dried *in vacuo* to give **18** (89.7 mg, 0.113 mmol, 89%) as a yellow powder. IR (HATR glaze):  $\nu_{\text{NO}} = 1597 \text{ cm}^{-1}$ . HRMS ( $m/z$ , obs(I); calc(I); error): 640.17041(20%); 640.17061(18%);  $-0.3 \text{ ppm}$ , 641.16747(91%); 641.16793(86%);  $-0.7 \text{ ppm}$ , 642.1704(80%); 642.17049(79%);  $-0.1 \text{ ppm}$ , 643.16957(100%); 643.17029(100%);  $-1.1 \text{ ppm}$ , 644.17336(42%); 644.17456(41%);  $-1.9 \text{ ppm}$ , 645.17232(84%); 645.17355(85%);  $-1.9 \text{ ppm}$ , 646.17541(20%); 646.17599(19%);  $-0.9 \text{ ppm}$ .  $^1\text{H}$  NMR (CDCl<sub>3</sub>,  $\delta$ ) (2:1): 7.97 (1H, d, Tp A), 7.95 (1H, d, Tp B), 7.82 (2H, d, Tp A + Tp B), 7.80 (3H, d, Tp A + 2Tp B), 7.72 (1H, d, Tp A), 7.68 (2H, d, Tp A + Tp B), 7.53 (1H, d, Tp A), 7.46 (1H, d, Tp B), 6.39 (1H, t, Tp A + Tp B), 6.37 (1H, t, Tp A + Tp B), 6.27 (1H, t, Tp A + Tp B), 4.80 (1H, dd ( $J = 9.1$ , 20.7), 5B), 4.48 (1H, dd ( $J = 7.9$ , 20.3), 5A), 4.34 (3H, s, 8A), 4.25 (3H, s, 8B), 4.22 (3H, s, 7A), 4.14 (3H, s, 7B), 3.90 (1H, m, 4B), 3.79 (1H, d ( $J = 2.3$ ), 5A), 3.70 (1H, t ( $J = 8.6$ ), 3A), 3.60 (1H, d ( $J = 10.7$ ), 5B), 2.41 (1H, d ( $J = 7.7$ ), 3B), 2.26 (1H, t ( $J = 7.9$ ), 4A), 1.22 (9H, d ( $J = 9.0$ ),  $\text{PMe}_3$  A), 1.20 (9H, d ( $J = 8.5$ ),  $\text{PMe}_3$  B).  $^{13}\text{C}$  NMR (CDCl<sub>3</sub>,  $\delta$ ): 194.7 (s, 2B), 193.6 (s, 2A), 186.6 (s, 6A), 185.6 (s, 6B), 144.0 (s, Tp), 143.7 (s, 2 Tp), 3.5 (s, Tp), 141.5 (s, Tp), 140.9 (s, Tp), 137.7 (s, Tp), 137.6 (s, Tp), 137.3 (s, Tp), 136.7 (s, Tp), 130.4 (s, Tp), 124.8 (s, Tp), 107.7 (s, Tp), 107.6 (s, Tp), 107.4 (s, 2 Tp), 106.5 (s, Tp), 106.3 (s, Tp), 58.8 (s, 7A), 58.0 (s, 7B), 57.9 (s, 8A), 57.6 (s, 4B), 57.4 (s, 8B), 52.9 (d ( $J = 1.7$ ), 4A), 48.7 (s, 3B), 47.6 (d ( $J = 6.3$ ), 3A), 34.7 (d ( $J = 3.4$ ), 5B), 32.9 (s, 5A), 12.7 (d ( $J = 30.5$ ),  $\text{PMe}_3$  B), 12.5 (d ( $J = 29.9$ ),  $\text{PMe}_3$  A).  $^{31}\text{P}$  NMR: (acetone- $d_6$ ,  $\delta$ ):  $-9.06$  ( $^{183}\text{W}$  satellite d ( $J = 275$ ),  $\text{PMe}_3$ ),  $-12.67$  ( $^{183}\text{W}$  satellite d ( $J = 267$ ),  $\text{PMe}_3$ ).

**TpW(NO)(PMe)<sub>3</sub>(3,4- $\eta^2$ -2-Methoxyppyridinium)(OTf) (10:1 A:B)**

**(19):** To a solution of **11** (216.9 mg, 0.3544 mmol) in DME (3 mL) was added pyridinium triflate (90.0 mg, 0.393 mmol, 1.1 equiv) in DME (1 mL). The reaction sat overnight (18 h) and crystals formed on the bottom of the reaction vessel. The crystals were collected on a medium porosity glass filter, washed with THF (5 mL) and hexanes (20 mL) and dried in vacuo to give **19A** (113.5 mg, 0.1489 mmol, 42%) as an orange powder. IR (HATR glaze):  $\nu_{\text{NO}} = 1591 \text{ cm}^{-1}$ . CV:  $E_{\text{p,a}} = +0.74 \text{ V}$ . HRMS ( $m/z$ , obs(I); calc(I); error): 610.15355(40%); 610.16004(18%);  $-10.6 \text{ ppm}$ , 611.1563(100%); 611.15735(86%);  $-1.7 \text{ ppm}$ , 612.15784(98%); 612.15991(79%);  $-3.4 \text{ ppm}$ , 613.15509(97%); 613.15968(100%);  $-7.5 \text{ ppm}$ , 614.15981(20%); 614.16402(40%);  $-6.9 \text{ ppm}$ , 615.16167(80%); 615.16295(85%);  $-2.1 \text{ ppm}$ , 616.16341(18%); 616.16536(19%);  $-3.2 \text{ ppm}$ .  $^1\text{H NMR}$  (acetone- $d_6$ ,  $\delta$ ): 11.19 (1H, br s, NH), 8.13 (2H, d, 2 Tp), 8.12 (1H, d, Tp), 8.05 (1H, d, Tp), 7.95 (1H, d, Tp), 7.66 (1H, d, Tp), 6.82 (1H, dd ( $J = 7.0, 6.6$ ), 5), 6.50 (1H, t, Tp), 6.45 (1H, t, Tp), 6.35 (1H, t, Tp), 6.07 (1H, d ( $J = 7.0$ ), 6), 4.44 (3H, s, 7 (OMe)), 3.73 (1H, dd ( $J = 10.6, 9.3$ ), 3), 2.28 (1H, dd ( $J = 9.3, 6.6$ ), 4), 1.30 (9H, d ( $J = 9.0$ ),  $\text{PMe}_3$ ).  $^{13}\text{C NMR}$  (acetone- $d_6$ ,  $\delta$ ): 175.4 (s, 2), 145.2 (s, Tp), 142.6 (s, Tp), 142.1 (s, Tp), 138.6 (s, Tp), 138.2 (s, Tp), 137.5 (s, Tp), 124.7 (s, 5), 113.2 (s, 6), 108.1 (s, Tp), 107.8 (s, Tp), 106.9 (s, Tp), 61.2 (s, 4), 58.0 (s, 7 (MeO)), 48.4 (d ( $J = 7.5$ ), 3), 13.2 (d ( $J = 29.9$ ),  $\text{PMe}_3$ ).  $^{31}\text{P}$ : (acetone- $d_6$ ,  $\delta$ ):  $-13.70$  (satellite d ( $J = 282$ ),  $\text{PMe}_3$ ).

**TpW(NO)(PMe<sub>3</sub>)(3,4- $\eta^2$ -(2-Dimethylaminopyridinium)) (20).** Compound **12** (99 mg, 1 equiv) was dissolved in THF (1 mL) and  $\text{CH}_3\text{CN}$  (3 mL), and then DPhAT (51 mg, 1.1 equiv) was added and stirred for 5 min. The solution was added to diethyl ether (75 mL), and the resulting precipitant was collected on a fine porosity frit and dried *in vacuo*. Isolated compound **20** (80 mg, 65% yield) as a beige solid.  $^1\text{H NMR}$  (acetonitrile- $d_3$ ):  $\delta$  8.05 (1, s, NH), 7.96 (1, d,  $J = 2.5$ , Tp), 7.94 (1, d,  $J = 1.9$ , Tp), 7.91 (1, d,  $J = 2.5$ , Tp), 7.89 (1, d,  $J = 2.12$ , Tp), 7.50 (1, d,  $J = 1.9$ , Tp), 7.41 (1, d,  $J = 2.2$ , Tp), 6.38 (1, t,  $J = 2.2, 2.5$ , Tp 4), 6.37 (1, t,  $J = 2.2, 2.5$ , Tp 4), 6.33 (1, t,  $J = 2.2, 2.5$  Hz, Tp 4), 6.1 (1, dd,  $J = 4.7, 6.9, 5$ ), 5.74 (1, dd,  $J = 4.7, 7.2, 6$ ), 3.67 (1, ddd,  $J = 4.7, 9.4, 14.1$  Hz, 4), 3.14 (3, s, NMe), 2.28 (3, s, NMe), 1.81 (1, d,  $J = 9.7, 3$ ), 1.25 (9, d,  $J = 8.7$ ,  $\text{PMe}_3$ ).  $^{13}\text{C NMR}$  (acetonitrile- $d_3$ ):  $\delta$  167.7 (s, 2), 145.4 (s, Tp), 143.2 (s, Tp), 141.9 (s, Tp), 138.5 (s, Tp), 138.4 (s, Tp), 138.3 (s, Tp), 115.1 (s, 6), 133.5 (d,  $J = 2.9$  Hz, 5), 107.8 (s, Tp 4), 107.7 (s, Tp 4), 59.9 (d,  $J = 11.7$  Hz, 4), 47.5 (s, 3), 39.7 (s, N-Me), 39.3 (s, N-Me), 13.2 (d,  $J = 29.9$  Hz,  $\text{PMe}_3$ ).

**TpW(NO)(PMe<sub>3</sub>)(4,5- $\eta^2$ -2-Trimethylsilylpyridinium)(OTf) (>20:1 kinetic) (21).** To a solution of **13** (113.5 mg, 0.1735 mmol) in DME (3 mL) was added pyridinium triflate (42.9 mg, 0.1873 mmol, 1.1 equiv) in DME (1 mL). The reaction was stirred overnight (18 h) and then added to stirred diethyl ether (50 mL). The resulting precipitate was collected on a medium porosity glass filter and dried in vacuo to give **21** (69.0 mg, 0.0858 mmol, 49%) as an orange powder. IR (HATR glaze):  $\nu_{\text{NO}} = 1600 \text{ cm}^{-1}$ . CV (DMA, TBAH, 100 mV/s, vs NHE):  $E_{\text{p,a}} = +0.76 \text{ V}$ . MS (ESI<sup>+</sup>):  $m/z = 654 [\text{M} - \text{H}]^+$ .  $^1\text{H NMR}$  ( $\text{CDCl}_3$ ,  $\delta$ ): 11.11 (1H, s, NH), 9.00 (1H, bs, 6), 7.91 (1H, d, Tp), 7.86 (1H, d, Tp), 7.84 (1H, d, Tp), 7.82 (1H, d, Tp), 7.71 (1H, d, Tp), 6.95 (1H, d ( $J = 5.5$ ), 3), 6.33 (2H, t (overlapping), 2 Tp), 6.27 (1H, t, Tp), 3.46 (1H, dd ( $J = 8.0, 11.7$ ), 5), 2.47 (1H, dd ( $J = 5.5, 8.0$ ), 4), 1.28 (9H, d ( $J = 8.5$ ),  $\text{PMe}_3$ ), 0.33 (9H, s, TMS).  $^{13}\text{C NMR}$  ( $\text{CDCl}_3$ ,  $\delta$ ): 163.9 (s, 6), 144.2 (s, Tp), 140.6 (s, Tp), 140.5 (s, Tp), 137.5 (s, Tp), 136.9 (s, Tp), 136.6 (s, 3), 136.1 (s, Tp), 127.3 (s, 2), 107.1 (s, Tp), 107.0 (s, Tp), 106.1 (s, Tp), 62.8 (s, 4), 59.6 (d ( $J = 5.8$ ), 5), 13.3, 12.9 (d ( $J = 29.9$ ),  $\text{PMe}_3$ ),  $-1.3$  (s, TMS).  $^{31}\text{P}$ : (acetone- $d_6$ ,  $\delta$ ):  $-16.17$  (satellite d ( $J = 286$ ),  $\text{PMe}_3$ ).

**TpW(NO)(PMe<sub>3</sub>)(4,5- $\eta^2$ -pyridine) (22).** To a solution of  $\text{TpW(NO)}(\text{PMe}_3)(\eta^2\text{-pyridinium})$  triflate (4:1 ratio of A to B) in acetone- $d_6$  was added an excess of NaH. The solution changed color immediately from orange to dark blue-green. The resulting spectrum showed **22** as well as the formation of  $\text{TpW(NO)}(\text{PMe}_3)(\text{pyridine})$  over time.  $^1\text{H NMR}$  (acetone- $d_6$ ,  $\delta$ ): two isomers (**22A** and **22B**) observed in a 4:1 ratio

(A:B): 8.75 (d,  $J = 4.3$  Hz, 1H, H2 A), 8.57 (d,  $J = 3.2$  Hz, 1H, H2 B), 8.05–8.18 (7H, Tp protons), 8.03 (d,  $J = 2.0$  Hz, 1H, Tp proton B), 7.93 (d,  $J = 2.0$  Hz, 1H, Tp proton B), 7.82 (d,  $J = 2.0$  Hz, 1H, Tp proton A), 7.64 (d,  $J = 2.0$  Hz, 1H, Tp proton A), 7.57 (d,  $J = 2.0$  Hz, 1H, Tp proton B), 6.79 (t,  $J = 6.3$  Hz, 1H, H5 B), 6.68 (t,  $J = 5.8$  Hz, 1H, H5 A), 6.47 (t,  $J = 2.0$  Hz, 2H, Tp protons A and B), 6.43 (t,  $J = 2.0$  Hz, 2H, Tp protons A and B), 6.40 (buried, 1H, H6 A), 6.35 (br, 1H, H6 B), 6.15 (t,  $J = 2.0$  Hz, 2H, Tp protons A and B), 4.01 (ddd,  $J = 13.1, 8.0, 5.8$  Hz, 1H, H4 A), 3.88 (ddd,  $J = 11.4, 9.4, 3.2$  Hz, 1H, H3 B), 2.34 (dd,  $J = 8.0, 4.3$  Hz, 1H, H3 A), 2.25 (m, 1H, H4 B), 1.32 (d,  $J = 8.9$  Hz, 9H,  $\text{PMe}_3$  A), 1.30 (d,  $J = 8.2$  Hz, 9H,  $\text{PMe}_3$  B).

**TpW(NO)(PMe<sub>3</sub>)(4,5- $\eta^2$ -pyridinium) Triflate (23).**  $\text{TpW(NO)}(\text{PMe}_3)(\eta^2\text{-benzene})$  (511.4 mg, 0.8801 mmol) was dissolved in a solution of pyridine (3.0 g) and pyridinium triflate (203.9 mg, 0.8904 mmol). After 5 h, the reaction solution was added to stirring hexanes to give an oil. Reduced pressure was used to remove all solvents. Attempts to precipitate a solid from DME or methylene chloride solutions also produced only oils. Addition of a THF solution of the product to a stirring mixture of ethyl ether and hexanes (80:20 by volume) precipitated a dark red orange solid. Rinsing the solid with chloroform gave **23** as a bright orange solid (87.9 mg, 0.120 mmol, 14% yield).  $^1\text{H NMR}$  (DMSO- $d_6$ ,  $\delta$ ): Isomer A: 11.96 (br, 1H, NH), 8.99 (t,  $J = 6.4$  Hz, 1H, H2), 8.21 (d,  $J = 2.0$  Hz, 1H, Tp proton), 8.19 (d,  $J = 2.0$  Hz, 1H, Tp proton), 8.08 (d,  $J = 2.0$  Hz, 1H, Tp proton), 8.04 (d,  $J = 2.0$  Hz, 1H, Tp proton), 8.02 (d,  $J = 2.0$  Hz, 1H, Tp proton), 7.78 (d,  $J = 2.0$  Hz, 1H, Tp proton), 6.86 (t,  $J = 5.9$  Hz, 1H, H5), 6.49 (t,  $J = 2.0$  Hz, 1H, Tp proton), 6.45 (t,  $J = 2.0$  Hz, 1H, Tp proton), 6.44 (t,  $J = 2.0$  Hz, 1H, Tp proton), 6.17 (dd,  $J = 4.0, 5.9$  Hz, 1H, H6), 3.98 (ddd,  $J = 12.3, 6.4, 5.9$  Hz, 1H, H4), 2.28 (t,  $J = 6.4$  Hz, 1H, H3), 1.18 (d,  $J = 8.9$  Hz, 9H,  $\text{PMe}_3$ ). Isomer B: 12.37 (br, 1H, NH), 8.98 (t,  $J = 6.4$  Hz, 1H, H2), 8.21 (d,  $J = 2.0$  Hz, 1H, Tp proton), 8.20 (d,  $J = 2.0$  Hz, 1H, Tp proton), 8.08 (d,  $J = 2.0$  Hz, 1H, Tp proton), 8.04 (d,  $J = 2.0$  Hz, 1H, Tp proton), 7.97 (d,  $J = 2.0$  Hz, 1H, Tp proton), 7.73 (d,  $J = 2.0$  Hz, 1H, Tp proton), 6.98 (t,  $J = 5.8$  Hz, 1H, H5), 6.48 (t,  $J = 2.0$  Hz, 1H, Tp proton), 6.43 (t,  $J = 2.0$  Hz, 1H, Tp proton), 6.40 (t,  $J = 2.0$  Hz, 1H, Tp proton), 6.10 (br m, 1H, H6), 3.75 (br m, 1H, H3), 2.24 (t,  $J = 5.8$  Hz, 1H, H4), 1.23 (d,  $J = 8.7$  Hz, 9H,  $\text{PMe}_3$ ).  $^{13}\text{C NMR}$  (DMSO- $d_6$ ,  $\delta$ ): Isomer A: 168.5 (s, C2), 145.3 (s, Tp carbon), 144.8 (s, Tp carbon), 141.8 (s, Tp carbon), 138.0 (s, Tp carbon), 137.5 (s, Tp carbon), 136.7 (s, Tp carbon), 126.4 (s, C5), 115.9 (s, C6), 107.4 (s, Tp carbon), 107.0 (s, Tp carbon), 106.8 (s, Tp carbon), 65.5 (d,  $J = 11.5$  Hz, C4), 57.5 (s, C3), 11.8 (d,  $J = 30.7$ ,  $\text{PMe}_3$ ). Isomer B: 163.6 (s, C2), 151.8 (s, Tp carbon), 144.5 (s, Tp carbon), 141.7 (s, Tp carbon), 140.6 (s, Tp carbon), 137.9 (s, Tp carbon), 137.4 (s, Tp carbon), 136.6 (s, Tp carbon), 129.0 (s, C5), 113.9 (s, C6), 107.3 (s, Tp carbon), 107.0 (s, Tp carbon), 106.3 (s, Tp carbon), 62.5 (s, C4), 59.5 (d,  $J = 5.8$  Hz, C4), 12.2 (d,  $J = 28.8$  Hz,  $\text{PMe}_3$ ).  $^{31}\text{P NMR}$ :  $-12.45 \text{ ppm}$  ( $J_{\text{PW}} = 294 \text{ Hz}$  for satellites). CV:  $E_{\text{p,a}} = 0.92 \text{ V}$ . IR:  $\nu_{\text{NO}} = 1592 \text{ cm}^{-1}$ .

**[TpW(NO)(PMe<sub>3</sub>)(pyridine)(H)] OTf (24).**  $\text{TpW(NO)}(\text{PMe}_3)(\eta^2\text{-benzene})$  (404.1 mg, 0.6955 mmol) was dissolved in pyridine (3.9 g). After 18 h, the pyridine was removed from the blue reaction solution under reduced pressure. A solution of DME (2.7 g) and pyridinium triflate (161.5 mg, 0.7052 mmol) was used to dissolve the resulting residue. A dark yellow solution resulted. The solution was left undisturbed for 1 h, allowing precipitation of **24** as a yellow solid, which was collected by filtration (222.0 mg, 0.3033 mmol, 44% yield).  $^1\text{H NMR}$  ( $\delta$ ): 12.42 (d,  $J = 121.3$  Hz, 1H, W–H), 8.19–8.32 (5H, 3 Tp protons and pyridine 2 and 6 protons), 8.18 (t,  $J = 6.7$  Hz, 1H, pyridine 4 proton), 8.02 (d,  $J = 2.0$  Hz, 1H, Tp proton), 7.63 (t,  $J = 6.7$  Hz, 2H, pyridine 3 and 5 protons), 7.23 (d,  $J = 2.0$  Hz, 1H, Tp proton), 6.63 (t,  $J = 2.0$  Hz, 1H, Tp proton), 6.59 (t,  $J = 2.0$  Hz, 1H, Tp proton), 6.24 (t,  $J = 2.0$  Hz, 1H, Tp proton), 1.63 (dd,  $J = 10.5, 0.5$  Hz, 1H,  $\text{PMe}_3$ ).  $^{31}\text{P NMR}$ : 5.32 ppm ( $J_{\text{PW}} = 147 \text{ Hz}$  for satellites). CV (in acetonitrile):  $E_{\text{p,a}} = 0.90 \text{ V}$ . IR:  $\nu_{\text{NO}} = 1608 \text{ cm}^{-1}$ .



**TpW(NO)(PMe<sub>3</sub>)(CO- $\eta^2$ -2,6-diacetylpyridine).** TpW(NO)(PMe<sub>3</sub>)-( $\eta^2$ -benzene) (100 mg, 0.172 mol) was dissolved in THF (0.8 mL) with pentane (4.0 mL) and 2,6-diacetylpyridine (281 mg, 1.72 mol, 10 equiv) and stirred for 18 h. The precipitate was collected on a fine porosity frit and washed with pentane (10 mL). Isolated compound: (60 mg, 52% yield) as a red/orange solid in a 1:1 ratio. CV:  $E_{p,a} = 0.99$  V. <sup>1</sup>H NMR (acetone-*d*<sub>6</sub>):  $\delta$  8.58 (1, d,  $J = 1.9$ , Tp), 8.42 (1, d,  $J = 1.9$ , Tp), 8.21 (1, d,  $J = 1.9$ , Tp), 8.18 (2, m, Tp), 8.05 (1, d,  $J = 1.9$ , Tp), 8.00 (1, d,  $J = 1.9$ , Tp), 7.96 (1, d,  $J = 2.3$ , Tp), 7.85 (1, d,  $J = 2.4$ , Tp), 7.84 (1, d,  $J = 2.4$ , Tp), 7.74 (1, dd,  $J = 7.3, 8.1, 4$ ), 7.66 (1, d,  $J = 2.1$ , Tp), 7.53 (2, m, Tp, 3 or 5), 7.50 (1, d,  $J = 1.1, 3$  or 5), 7.19 (1, d,  $J = 7.9, 3$  or 5), 7.18 (1, d,  $J = 7.9, 3$  or 5), 6.42 (1, t,  $J = 2.3, 2.23$ , Tp 4), 6.36 (1, t,  $J = 2.1, 2.3$ , Tp 4), 6.35 (1, t,  $J = 2.1, 2.3$ , Tp 4), 6.34 (1, t,  $J = 2.3$ , Tp 4), 6.22 (1, t,  $J = 2.3$ , Tp 4), 6.18 (1, t,  $J = 2.3$ , Tp 4), 2.74 (3, d,  $J = 1.9$ , Me (bound)), 2.72 (3, s, Me (unbound)), 2.62 (3, d,  $J = 1.1$ , Me (unbound)), 1.70 (3, d,  $J = 9.2$ , Me (bound)), 1.48 (9, d,  $J = 9.4$ , PMe<sub>3</sub>), 1.41 (9, d,  $J = 9.3$ , PMe<sub>3</sub>). <sup>13</sup>C NMR (acetone-*d*<sub>6</sub>):  $\delta$  200.7 (CO (unbound)), 200.6 (CO (unbound)),

173.4 (6), 169.4 (6), 152.0 (2), 151.8 (2), 147.7 (Tp), 145.1 (Tp), 144.9 (Tp), 144.6 (Tp), 144.2 (Tp), 137.1 (Tp), 137.0 (Tp), 136.7 (Tp), 136.1 (Tp), 135.9 (4), 125.2 (Tp), 122.6 (3 or 5), 122.3 (3 or 5), 116.6 (3 or 5), 116.8 (3 or 5), 107.4 (Tp 4), 107.0 (Tp 4), 106.4 (Tp 4), 106.3 (Tp 4), 105.8 (Tp 4), 105.6 (Tp 4), 28.5 (Me (unbound)), 25.8 (Me (bound B)), 25.6 (Me (unbound)), 21.0 (Me (bound A)), 11.27 (d,  $J = 27.47$  Hz, PMe<sub>3</sub>), 11.00 (d,  $J = 27.7$  Hz, PMe<sub>3</sub>).

**Acknowledgment.** Acknowledgment is made to the NSF (CHE- 0116492 (UR)) and the NIH (NIGMS: R01-GM49236 (UVA)) for financial support of this work.

**Supporting Information Available:** Crystallographic details for compound **21B**, spectra for selected compounds, and the complete reference 26. This material is available free of charge via the Internet at <http://pubs.acs.org>.

JA066623F